1986

Composite beam test with formed metal decking and cellular raceways /

Joseph Marinaccio Jr.
Lehigh University

COMPOSITE BEAM TEST WITH FORMED METAL DECKING AND CELLULAR RACEWAYS

by

Joseph Marinaccio Jr.

A Thesis

Presented to the Graduate Committee

of Lehigh University

in Candidacy for the Degree of

Master of Science

in

Civil Engineering

Lehigh University

April 1986

Certificate of Approval

This thesis is accepted and approved in partial fulfillment of the requirements for the degree of Master of Science.

April 26, 1986
(date)

Roger G. Slutter
Professor in Charge

Irwin J. Kugelman
Chairman of Department

TABLE OF CONTENTS

LIST OF TABLES

LIST OF FIGURES

ABSTRACT

This report summarizes a study to determine the strength and behavior of steel concrete composite beams with formed metal decking and cellular raceway panels, and to evaluate the fourth provision of the AISC specification 1.11.5.2 which deals with resisting uplift.

This study is based on the test of a composite beam composed of a W16X57 A36 steel beam, and a concrete slab with a design strength of 24 MPa. and a thickness of 63.5 mm above the ribs. The metal decking was 20 gauge galvanized steel with embosements, and a rib height of 76.2 mm. The shear connectors were 19 mm diameter studs embedded 38 mm above the height of the ribs. The composite beam was simply supported on a span of 10.1 m.

The characteristics of load applied to the beam as a function of mid-span deflection, steel strains at mid-span, and slips of the slab relative to the steel beam at various locations along the span are reported. The results of this test indicates that satisfactory composite behavior may be developed with the AISC 406 mm maximum shear connector spacing increased to 610 mm at the locations of a cellular raceway

1. INTRODUCTION

Composite construction utilizing formed steel decking has been in use since the early 1960's. Since then many studies have been carried out to evaluate their behavior.

The first studies tried to relate the beams designed with steel decking to that of beams designed with flat soffit slabs which were well understood at that time. In 1967 Robinson[1] concluded that beams designed with high narrow ribs significantly reduced the shear capacity of the studs. He also suggested that the strength of the connectors is proportional to the rib geometry. A few years later Fisher[2] summarized the available test data and concluded that a ribbed slab could be modelled as a haunched slab, with the slab force acting at the centroid of the solid portion of the slab.

In 1977 test results[3] were published for a series of full size composite beams with steel formed decking and various rib geometry. From these tests a method for predicting shear stud capacity was established based on rib width, stud height and the number of connectors in a rib. Shortly after this a paper[4] modified a few other methods for predicting load deflection diagrams, to obtain

a way of predicting the complete load deflection diagram. Grant[4] also showed that a connector developes a peak load and then gradually falls off in a ductile manner.

The purpose of this study will be to report the results of a composite beam test utilizing formed steel decking and cellular raceways, and attempt to explain the results obtained.

By introducing a cellular raceway into the decking a rib is lost where each raceway panel is placed. The effect of losing a rib for each panel placed could significantly reduce the amount of shear connection developed if too many panels are used or if these panels are placed in areas of high horizontial shear forces. Another problem with the cellular raceway is that one is forced to violate the AISC[5] code for the spacing of shear connectors. The fourth provision of the specification 1.11.5.2 requires that in order to resist uplift the steel decking shall be anchored to all compositely designed steel beams at a spacing not to exceed 406 mm. Therefore if a cellular raceway panel is used with a width greater than 406 mm this provision will be violated as is the case of the beam test described in this thesis.

2. DESCRIPTION OF TEST

2.1 Test Program

The test program reported consisted of one simple span composite beam with formed steel decking and cellular raceway panels.

2.2 Test Specimen

The test specimen consisted of a composite steel and normal weight concrete beam with formed steel decking and cellular raceways supported on a simple span of 10.1 m. Details of this beam can be seen in figure 1. A photograph of the test specimen before testing is shown in figure 2.

The Steel section choosen for this beam was a W16X57. The concrete slab dimensions were 140 mm by 2.44 m in cross-section. Slab reinforcement consisted of 6X6-#10/#10 welded wire fabric which was placed at mid-depth of the 63.5 mm thick solid slab. figure 3 shows the slab reinforcement before casting the slab. The concrete slab was cast without shoring.

The metal decking used to cast the slab consisted of Walker 209 cellular raceway panels and Wheeling Super-bond 300. Both types of decking had embossements and were fabricated from 20 gauge galvanized steel material in

widths of 610 mm. The rib height of test specimen was 76 mm, with a spacing of 305 mm, and a width to height ratio of 2.0. The Walker raceways panels were located 1.83 m and 4.27 m in from each end of the 10.36 m test beam. See figure 4 for decking and raceway locations.

Composite action between the steel beam and the concrete slab was provided by the placement of 19 mm diameter headed studs. The stud shear connectors were all embedded in the concrete slab 38 mm above the top of the ribs. The connector locations and spacing can also be seen in figure 4, and figure 5 shows the headed studs before the slab was cast.

2.3 Control Tests

In order to determine the mechanical properties of the elements which composed the composite beam, control test of the elements were conducted. For each of the elements a description of the tests conducted and the results follows.

2.3.1 Steel Beam

The properties of the ASTM A36 W16x57 section used for fabrication of the composite beam specimen was determined from standard tensile test specimens. Coupons were machined from a 610 mm section, flame cut from near the support. A total of four coupons were taken, two from the web and two from the bottom flange.

Results from the steel tensile coupon tests are reported in Table 1. The yield strengths of the coupons machined from the web were higher than those obtained from the bottom flange, which is common in rolled products. The static yield stress was used in the analysis of the composite beam, because it approximates the steel strength expected from the member due to the slow rate of loading during the testing. The measured yield stress was approximately 20% higher than that anticipated. The modulus of elasticity of the steel was taken as 200 Gpa.

2.3.2 Concrete Slab

The concrete used for the slab was normal weight concrete conforming to the ASTM standard C33. During the process of casting the slab seven standard 152 mm by 305 mm control cylinders were cast so that the compressive strength, modulus of elasticty and tensile strength of the concrete could be determined. The slab and cylinders were both moist cured for fourteen days, then stripped and air cured until the day of testing.

The cylinders to be used for determining the compressive strength were capped with a sulfur compound and tested according to ASTM Standard C39 (Standard Method of Test for Compressive Strength of Molded Concrete Cylinders). Five of the seven cylinders cast were used to determine the compressive strength. During the curing of

the concrete two cylinders were used to determine the compressive strength at fourteen days and twenty eight days. The remaining three cylinders were tested the day of the composite beam test.

The modulus of elasticity of the concrete was determined from the compression test of the cylinders. The strain in the cylinder was measured using a 152 mm gage length compressometer mounted on the cylinder. During the cylinder test the dial gage readings were recorded at each load increment of 22.3 KN or a stress increment of 1.22 MPa. The modulus of elasticity was then calculated from a linear regression using the readings between 22.3 KN and 334.5 KN on the second cycle of loading to 50% of ultimate. However, if the modulus of elasticity was taken as the tangent modulus at zero a sligthly higher value may have been realized.

The tensile strength of the concrete was determined from split cylinder tests in accordance with ASTM Specification C496 (Methods of Test for Splitting Tensile Strength of Molded Concrete Cylinders). The remaining two of the seven cylinders were used to obtain the tensile strength of the concrete. These cylinders were also tested during the day of the composite beam test.

The results of the concrete cylinder control tests are listed in Table 2. In all analysis where the concrete

properties are required, the average of the values obtained from the proper control tests were used.

2.3.3 Stud Shear Connectors

The stud shear connectors conformed to the ASTM A108 specifications and were welded directly through the metal decking to the upper beam flange in a staggered pattern using a stud welding gun. All of the welds were tested by "sounding" the studs with a heavy hammer. Any questionable studs were given a 15 degree bend test. Faulty studs were replaced and retested. No other control tests were preformed in order to determine the mechanical properties of the studs.

2.3.4 Slab Reinforcement

The 6X6-#10/#10 welded wire fabric used for temperature and shrinkage control in the slab conformed to ASTM A185-64 specifications. No control tests were performed on the reinforcement.

2.4 Instrumentation

The instrumentation used on the composite beam specimen consisted of electrical resistance strain gages, for strain measurement, and dial gages, for slip and deflection measurements.

Six strain gages were symmetrically placed about the web at the mid-span of the beam. Two gages were placed on the bottom side of each flange, and the remaining two were

placed on the web at mid-height as can be seen in figure 6. The gages on the opposite side of the web were averaged so that the strain in the steel section could be obtained at that particular location. The strain gage readings will also be used to determine the strain in the concrete slab at mid-span.

Four of the five 254 μm dial gages were used to measure the relative slip of the steel to the concrete, and the remaining gage was used to measure deflections. One dial gage was placed at each end of the test specimen in order to measure the slip between the top flange and the concrete slab. The remaining dial gages were placed approximately 1.9 m in from each end of the beam, which would place them directly behind the cellular raceway panels closest to the ends. These gages were clamped to the upper flange and measured the movement of a small angle epoxied to the cellular raceway in order to obtain the slips.

2.5 Test procedure

A four point loading system was used to provide shear and moment conditions comparable to uniform loading conditions, as can be seen in figure 7. The load was distributed to four transverse spreader beams equally spaced at 2.44 m so that the load would be applied directly over a rib. This was accomplished by using three

simply supported spreader beams. In order to obtain a uniform bearing on the slab a sheet of 12.7 mm Homosite was placed under each transverse spreader beam. The load was applied hydraulically to the beam specimen using the 22.2 MN testing machine at the Fritz Engineering Laboratory, Lehigh University.

All of the measurements taken during the testing process, unless otherwise stated do not account for the dead load (steel beam self-weight, concrete weight and the six small spreader beams used to apply the loads). The approximate dead load was 72.4 KN.

The first load increment applied to the composite beam specimen was 19.4 KN which was obtained by lowering the large spreader beam onto the two smaller spreader beams. After this was accomplished small load increments of 22.2 KN were applied until a working load of 241.8 KN was obtained. Once the working load was obtained the beam was unloaded to 41.6 KN and cycled between 41.6 KN and 241.8 KN for a total of ten times. After the tenth cycle the beam was loaded to near ultimate load, in 22.2 KN increments. At load levels near ultimate, load relaxation occured and readings were taken once the test specimen stabilized. The load recorded was the maximum obtained. Once the plateau of the load deflection curve was reached, deflection increments rather than load increments were

used for load application. Loading was terminated once the deflections became excessive. The maximum mid-span deflection obtained was 129 mm.

3. TEST RESULTS

3.1 Beam Behavior

The composite beam specimen was cycled ten times between 41.6 KN and a working load of 241.8 Kn. During the cycling no significant or unusual results were obtained between each cycle. After the tenth cycle the beam specimen was continued to be loaded in increments of 22.2 KN. When the load had reached approximately 400 KN signs of yielding were noticed on the bottom flange as the mill scale had started to flake off. As the loading continued the yielding began to extend into the web region.

A longitudinal crack was discovered on the slab surface at a load of 465 KN which extended from the east end of the slab to about mid-span. This crack was located directly above the web of the steel beam. As the loading continued the crack propagated towards the west end of the slab, which it reached at approximately 575 KN.

Another crack began to initiate at the west end of the beam specimen at a load of 486 KN. This crack started out at mid-height of the solid portion of the slab directly above the web, and as loading progressed the

crack was pulled towards the steel beam at an angle of approximately 45 degrees. Figure 8 shows the crack at the conclusion of the test. Once this crack had formed the bond between the concrete and the last sheet of metal decking on the west end began to separate. Figure 9 shows this separation at the conclusion of the test.

At a load of 589 KN the test was stopped and the beam was unloaded. At the conclusion of the test the areas adjacent to the Walker cellular raceway panels were thoroughly inspected for any signs of cracking or bond separation, but none were found. Figure 10 shows the Walker panels before testing and figure 11 at the conclusion of the test.

3.1.1 Beam Deflections

A graph of the applied load versus mid-span deflection can be seen in figure 12. The deflection at the working load of 241.8 KN was 18 mm. And a deflection of 129 mm was obtained at the ultimate load. After the beam was unloaded the mid-span permanent set was 88 mm.

3.1.2 Steel Strains

The strain in the steel beam due to the applied load was monitored at three locations, bottom flange, mid-height of the web, and the top flange. Figures 13-15 shows the applied load versus strain for each of the three locations. At the working load the strain in the bottom

flange was 722 micro mm/mm, the web 356 micro mm/mm, and the top flange 22.6 micro mm/mm. Figure 13 clearly shows yielding of the bottom flange at approximately 400 KN. however, figure 14 does not show a clear indication of yielding, but yielding most likely occured around 425 KN. From figure 15 it is very difficult to pinpoint any location where yielding occured, if any did occur.

3.1.3 Relative Slip

The slips obtained in the west shear span at the end of the beam and those behind the cellular raceway panels are plotted as load versus slip in Figures 16 and 17, respectively. Also, the slips obtained in the east shear span at the same locations are plotted in Figures 18 and 19. At the working load of 241.8 KN the slip measured at the ends of the beam were 102 μm for the west end and 178 μm for the east end. Also, at the working load level the slip behind the west cellular raceway panel was 50 μm. and behind the east panel 102 μm. During the cycling of the test beam the slips increased by approximately 25 μm. Near ultimate load the slips increased very rapidly at all of the slip gage locations, except at the location of the east cellular panel raceway panel, as can be seen in the figures. At the ultimate load the slips measured at the ends were 2.77 mm for the west end, and 3.05 mm for the east end. Also, the slip behind the west raceway panel was

3.73 mm, and 0.94 mm behind the east raceway panel. After unloading the test specimen the permanent slip deformations were 2.13 mm, 3.05 mm, 3.73 mm, and 0.61 mm for the west end, east end, west panel, and east panel locations respectively.

3.2 Cellular Raceway Behavior

The cellular raceway panels used in the test specimen showed no signs of cracking or debonding during the cycling process. As the beam was loaded to failure the cellular raceway panels still did not show any signs of debonding, cracking, or uplift. Once the ultimate load was reached the cellular raceway panels were thoroughly inspected before the test specimen was unloaded, and still no signs of damage were detected.

4. ANALYSIS OF COMPOSITE BEAM

4.1 Composite beam design

The composite beam specimen was designed in accordance with the AISC specifications[5] for composite beams, section 1.11. The maximum amount of shear connectors that could be used was limited by the number of ribs available. A 58.6% shear connection was obtained by placing two headed studs per rib. The section properties of the composite beam were calculated using the above specifications, and using these properties the section modulus was calculated. By using AISC formula 1.11-1 an effective section modulus was obtained to account for the partial shear connection.

The working load moment calculated using the AISC specification assuming a yield stress of 248 MPa was, 410 KN-m. This moment would correspond to an applied load of 247.8 KN, which was approximately the load applied by the testing machine during the cycling process. If the actual material properties were known before the testing began a higher working load could have been used.

The ultimate moment was calculated by the method suggested by Slutter and Driscoll[6] for composite beams.

The slab force was assumed to be equal to the number of connectors in the shear span multiplied by the ultimate load for a connector, which was taken as two times the design load. This force was then assumed to act at the centroid of the solid portion of the concrete slab above the top of the ribs. And using the same section properties used to calculate the section modulus, the ultimate strength obtained was 910 KN-m. The ultimate strength obtained from the test data was 852 KN-m, which includes the dead load, corresponds to a 6% difference.

Using the working load moment calculated according to the AISC specifications, and the ultimate moment obtained from the test, a ratio of ultimate to working load of 2.07 was obtained. A value that is greater than 2.0 would indicate a good measure of ductility or reserve capacity.

4.2 Beam Deflections

Using the AISC formula 1.11-6 an effective value for the moment of inertia was calculated to account for the amount of shear connection provided. Now by appling the virtual work equation and substituting the modulus of elasticity and the effective moment of inertia a relationship for the deflection as a function of load was obtained in the elastic region. Figure 20 shows the theoretical load-deflection curve as a solid line and the experimential results as points. From this figure it can

be seen that the beam acted stiffer than that predicted over the range of 352 KN. The theorectical deflection at the working load of 241.8 KN was 20 mm as compaired to the actual deflection of 18 mm, which corresponds to a 6% difference.

4.3 Connector Slip Behavior

Slip occurs between the concrete slab and the steel beam in all composite beams. The slip is caused by the incomplete interaction of the discretely placed shear connectors which are not infinitely rigid. Figures 16 and 17 show the load versus slip for the west shear span. From these figures up to the ultimate plateau the slip at the raceway panel is less than that at the end of the beam. However, once the plateau is reached the slip at the raceway panel increases faster than that at the end of the beam. An explaination of why the slip along the beam was greater than that of the end, can be seen by examing figure 8. From carefull examination of the cracked surface and the location of the dial gage it can be concluded that the movement of the slab above the crack must have been greater than that below the crack. And since the dial gage was located below the crack, smaller movements were record.

Figures 18 and 19 show the load verus slip for the east shear span. Looking at these figures it can be seen

that the slip behind the raceway panel is much less than the slip at the end of the beam. Also, it can be seen that the slip at the end of the beam does not progress linearly up to a level plateau as the others do. A possible cause of this could be the way in which the beam was supported, because the east end was a fixed support and the west end was an expansion support, or due to the possible unsymetrical placement of the loads as ultimate was neared.

4.4 Slab force

The slab force at mid-span was determined by measuring the strain profile on the steel section at mid-span. The strain profile was then converted into stresses and integrated to obtain the net force and moment in the steel beam. The slab force was then found from equilbrium. Also, from the strain profile the location of the neutral axis could be determined. Figure 21 shows a typical strain profile and the position of the neutral axis.

Examing the strain profiles and the position of the neutral axis over the range of 300 to 400 KN it can be seen that as the load is increasing the neutral axis is shifting downward. This would explain why figure 15 shows an increase in load, but very little change in strain over this range. The cause of this shifting is due to the

redistribution of load due to the yielding of the steel section.

4.5 Finite Element Model

A finite element model was developed to study the effects of the cellular raceway panel on the shear connectors and the overall beam behavior. Also this model was used to study the effects caused by placing the raceway panels at different locations along the beam. The finite element program used for the analysis was SAP IV. Figure 22 shows a plot of the finite element mesh, and figure 23 shows the same plot with the slab removed and the shear connectors numbered.

4.5.1 Element Types

The concrete slab was modelled using plate bending elements with membrane capabilities. The slab was divided into eight strips of 305 mm square elements 63.5 mm thick along the length of the slab. Only the solid portion of the slab above the ribs was modelled because the ribs do not contribute to the bending stiffness of the composite beam for the major bending. All of the concrete properties obtained from the control cylinders were used for the element properties.

The steel beam was modelled using plane stress elements for the web and beam elements for the flanges. The web was divided into three strips of 133 mm by 152 mm

plane stress elements along the length of the beam. The top and bottom flanges were divided into 152 mm lengths for the beam elements. All of the physical and material properties were obtained from the proper control tests for that element.

The shear connectors were modelled as beam elements connected to the top flange and the concrete slab. The properties used for these elements were those of the concrete, because the strength of the shear connectors is based upon the strength of the concrete.

4.5.2 Boundry Conditions

Due to the symmetry of the composite beam only one half of the beam needs to be analyzed. In order to do this certain boundry conditions must be placed on the cut section. These conditions will only allow vertical displacements and rotations about the longitudinal axis in order to simulate the full beam. The boundry conditions at the support will only restrict the vertical movements.

4.5.3 Loading Conditions

Concentrated forces were placed 1.37 and 3.81 m in from the end of the slab to simulate the loading conditions used during the test. The asterisks in figure 22 indicates the nodes where the concentrated forces were placed.

4.5.4 Model Verifications

The finite element model with shear connectors 8 and 16 removed was verified by checking the stresses and reactions against those obtained from the test results for a few load increments in the elastic range. All of the results obtained from the finite element model corresponded very closely to those from the test, so the model was considered to be a realistic representation.

4.6 Finite Element Analysis

Once the model was verified with the test results, shear connectors were removed at various locations along the beam to study the effects on the remaining connectors. The first series of analysis consisted of removing just one connector and studying the effects, replacing it and removing another until each connector was removed once. The next series consisted of essentially the same procedure as the first series, except now two adjacent connectors were removed each time. The final series consisted of removing various connectors along the beam to simulate the different possible locations of the cellular raceway panels.

4.6.1 Results

The shear connector force distribution obtained from the finite element model with connectors 8 and 16 removed to simulate the composite beam tested, is shown in figure

24. And figure 25 shows the distribution obtained with no missing connectors. By examming these two distributions it can be seen that connectors 3,4 and 5 are the most highly stressed and the shear forces on connectors 1 and 2 near the end of the beam are much less. Also, as a result of removing connectors 8 and 16 the shear forces on connectors 5 through 12 increased by at least 4.5 KN each, and connectors 6,7,9 and 10 increased by approximately 8.0 KN each.

The result obtained from the first series of analysis in which one connector at a time is removed, was plotted as a series of bar graphs representing the forces on each connector resulting from the removal of one connector. Figure 26 shows a typical graph of the shear force on connector 4. Studying these graphs it can be seen that when one connector is removed the shear force on the four surrounding connectors (two on each side of the removed connector) are the most affected. But when the connector is removed from an area of low shear forces such as mid-span the effect is much less pronounced.

The results obtained from the second series of analysis where two adjacent connectors were removed was plotted the same as above. Figure 27 shows a typical graph of the shear forces on connector 4 from the removal of two connectors at a time. Studying these graphs the same

effects caused by removing only one connector occurs, but one more connector on each side of the removed connector is affected and the increase in shear is much greater as can be seen in the above figure. Also of interest is the phenomenon that occurs and is shown in figure 28. This figure shows that the forces on connector 8 are the highest when connectors 5 and 6 are removed, but the removal of the adjacent connectors 6 and 7 does not affect the shear forces as much. This trend occurs on the connectors between 5 and 17.

The last series of analysis in which various connectors were removed in order to simulate the possible locations of the cellular raceway panels showed basically what was expected. When the shear connectors were removed near mid-span the effect on the shear force distribution was very small. But, when the connectors near the ends were removed the effect on the distribution was very large. Figure 29 shows two shear distributions; the upper was obtained when one raceway was placed near the end, and the lower from the placement of two consecutive raceway panels near the ends. From these distributions it can be seen that by placing one raceway panel near the end the shear forces on the first six connectors increases. And when two raceways are placed side by side the shear forces become very large especially on the connector between the

two panels.

From the three series of analysis it can be concluded that when a cellular raceway panel must be used, it is advisable to place them in areas of low horizontial shear. And, if two cellular raceway panels must be placed next to each other they should not be located near the ends.

5 SUMMARY AND CONCLUSIONS

This study presents the results of a composite steel concrete beam with formed metal decking and cellular raceways. The purpose of this investigation was to evaluate the fourth provision of the AISC specification[5] 1.11.5.2 which deals with resisting uplift; and to suggest possible locations for the cellular raceways.

The composite beam tested consisted of a W16X57 beam of ASTM A36 steel acting compositly with a concrete slab. The slab was cast on 20 gauge galvanized steel decking with a constant 63.5 mm thick concrete slab above the top of the 76.2 mm high ribs. Minimal reinforcement of 6X6-#10/#10 welded wire fabric was placed at mid-height of the solid slab portion. The shear connectors were 19 mm diameter shear studs embeded 38 mm above the ribs. Spacing of the shear connectors were 305 mm except at the cellular raceway in which case the spacing was 610 mm.

The results of the composite beam test incorporating cellular raceways indicates that the requirements of AISC specification 1.11.5.2 paragraph A need not be met when cellular raceway panels of the type used in this test are utilized. The cellular panel is rigid enough to span the

width of the panel between tie down points without separation from the steel beam. Bond failure was not observed near any of the cellular raceway panels indicating that the panels retain their initial shape throughout the test. The closed shape of the cellular panel exhibits adequate rigidity to permit a shear connection or tie down spacing of 610 mm. The location of the raceways used in this test was selected as being typical for composite construction. Other arrangements of the raceways may result in a less satisfactory behavior of the composite beam. However, this would be due to the less favorable arrangement of shear connectors rather than the 406 mm spacing of connectors at the cellular raceway panels.

6. TABLES

TABLE 1 - STEEL PROPERTIES

Specimen	Area (mm)	Yield Stress (KPa)	Ultimate Stress (KPa)	Percent Elongation (%)	Reduction in area (%)
WEB-1	450	377	490	19.4	53.4
WEB-2	460	308	449	31.5	52.3
FLANGE-1	597	302	463	27.5	55.8
FLAMGE-2	611	290	442	27.3	60.1
AVERAGE WEB	455	342	470	25.5	52.9
AVERAGE FLANGE	604	296	453	27.4	58.0

TABLE 2 - CONCRETE PROPERTIES

Compressive Strength test

Age (days)	Cylinder Number	Ultimate Load (KN)	f'_c (MPa)	E (GPa)
14	1	549	30.1	-
28	2	578	31.7	-
day of test				
35	3	601	32.9	26.0
35	4	627	34.4	26.0
35	5	609	33.4	25.7
	Average	612	33.6	25.9

Split Cylinder test

Age (days)	Cylinder Number	Ultimate Load (KN)	Tensile Strength (MPa)
35	6	262	3.60
35	7	262	3.60

7. FIGURES

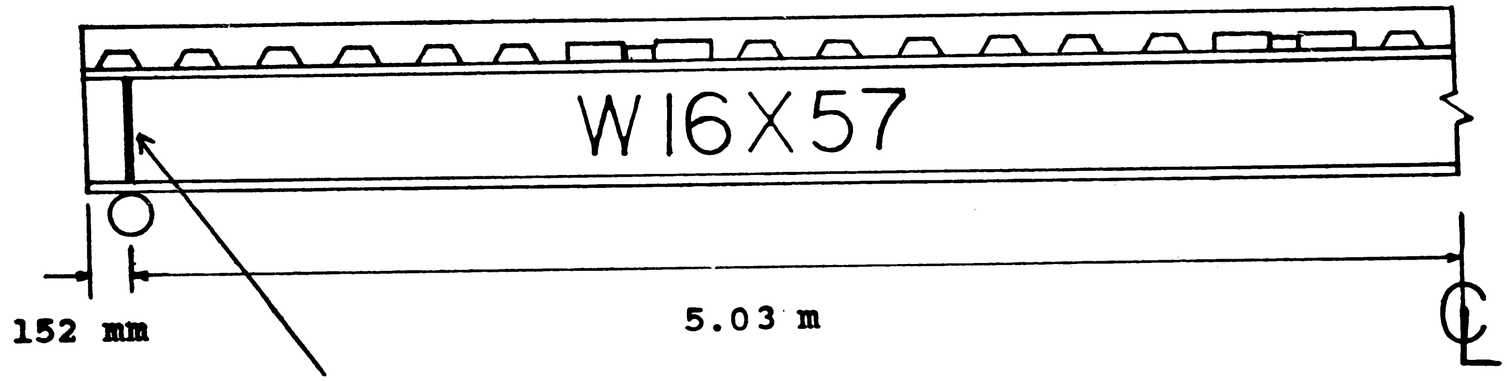

Figure 1: Test Specimen Details

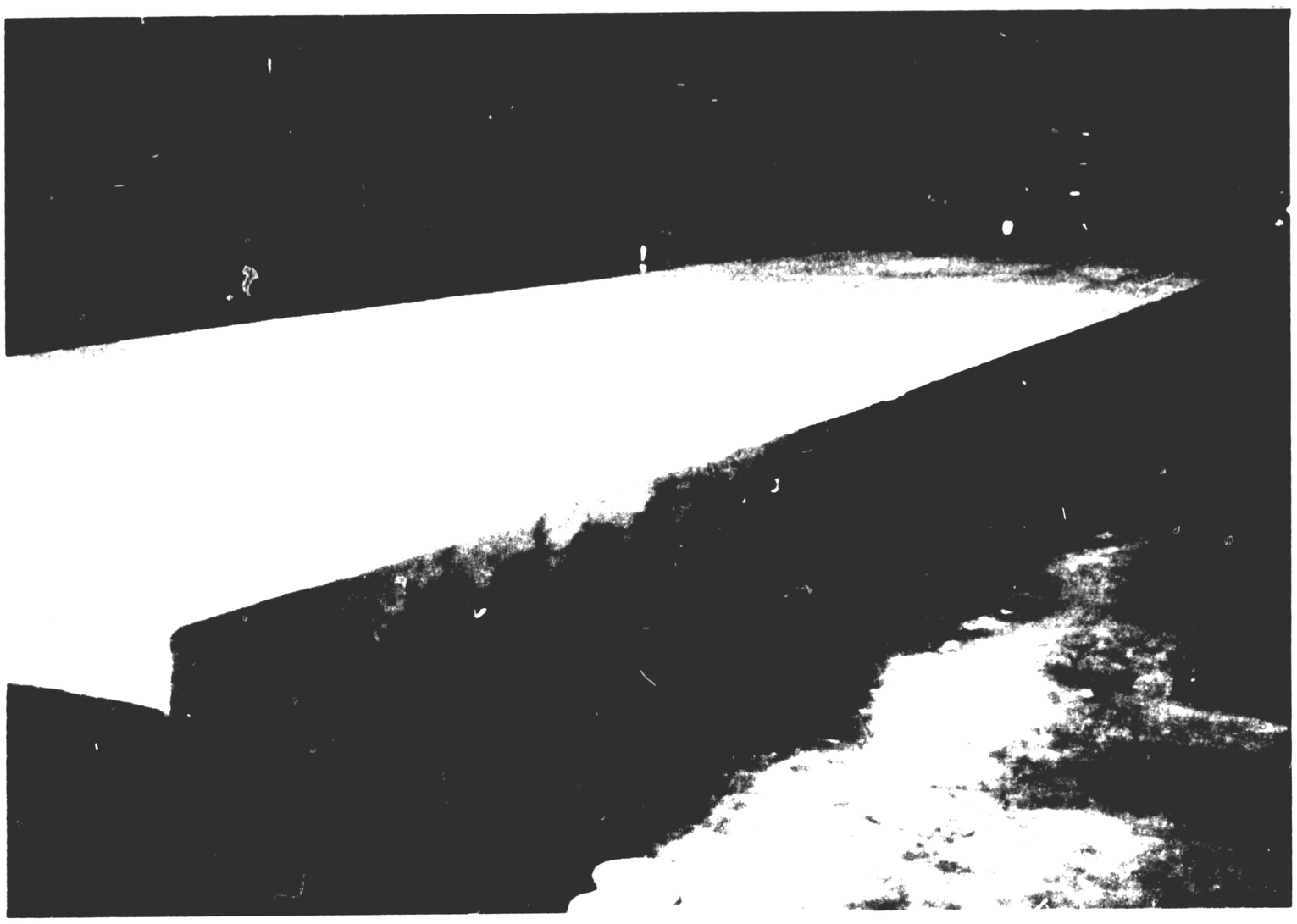

Figure 2: Test Specimen Before Test

Figure 3: Slab Reinforcement

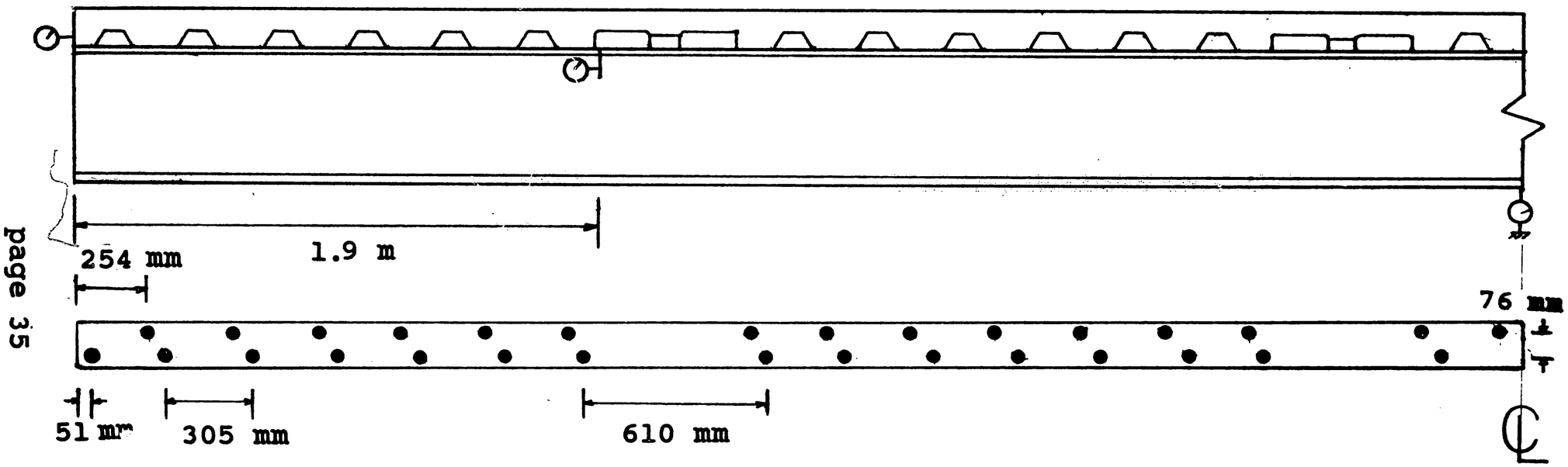

Figure 4: Shear Connector and Dial Gage Locations

Figure 5 Shear Connectors Welded Through Metal Decking

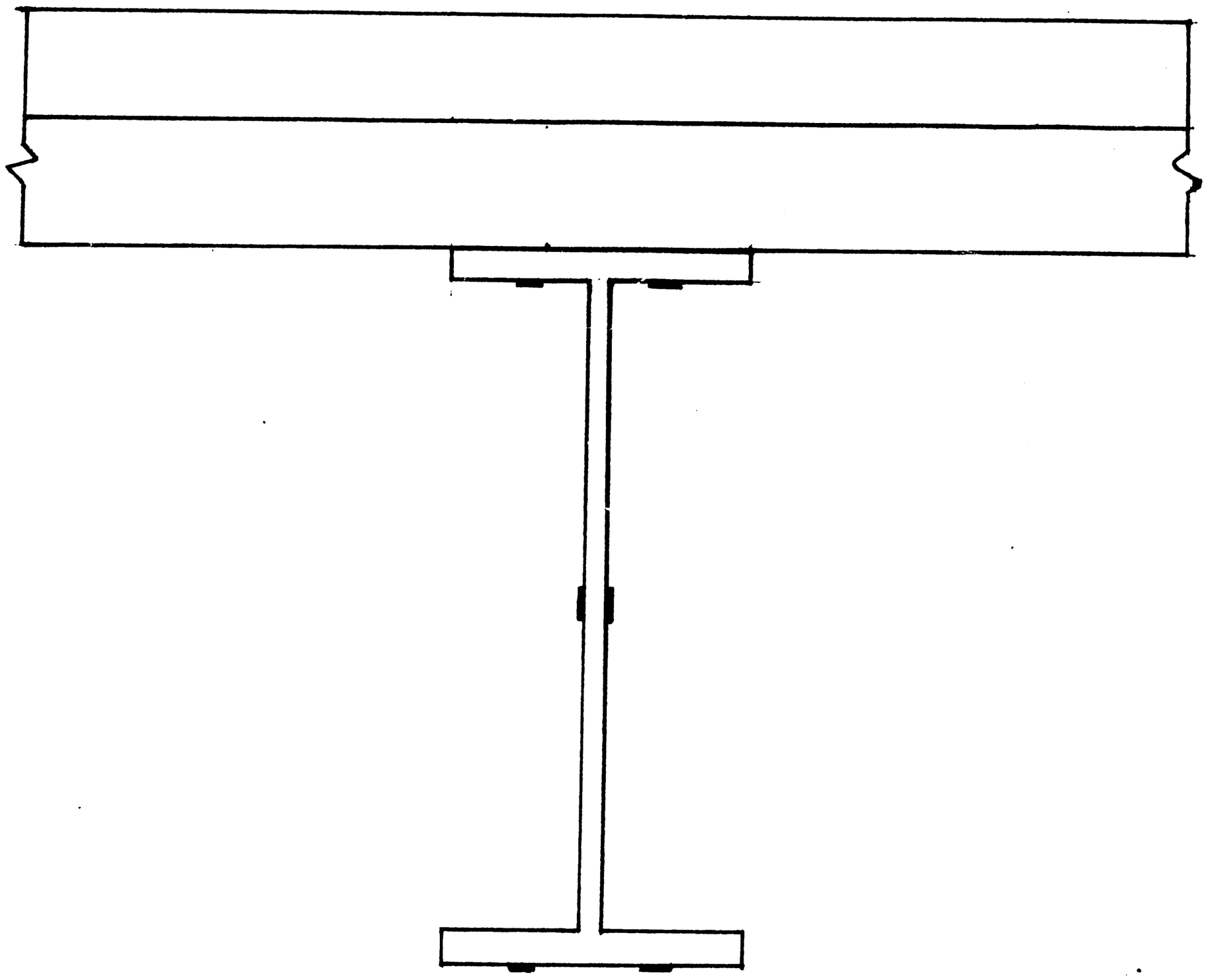

Figure 6: Strain Gage Locations

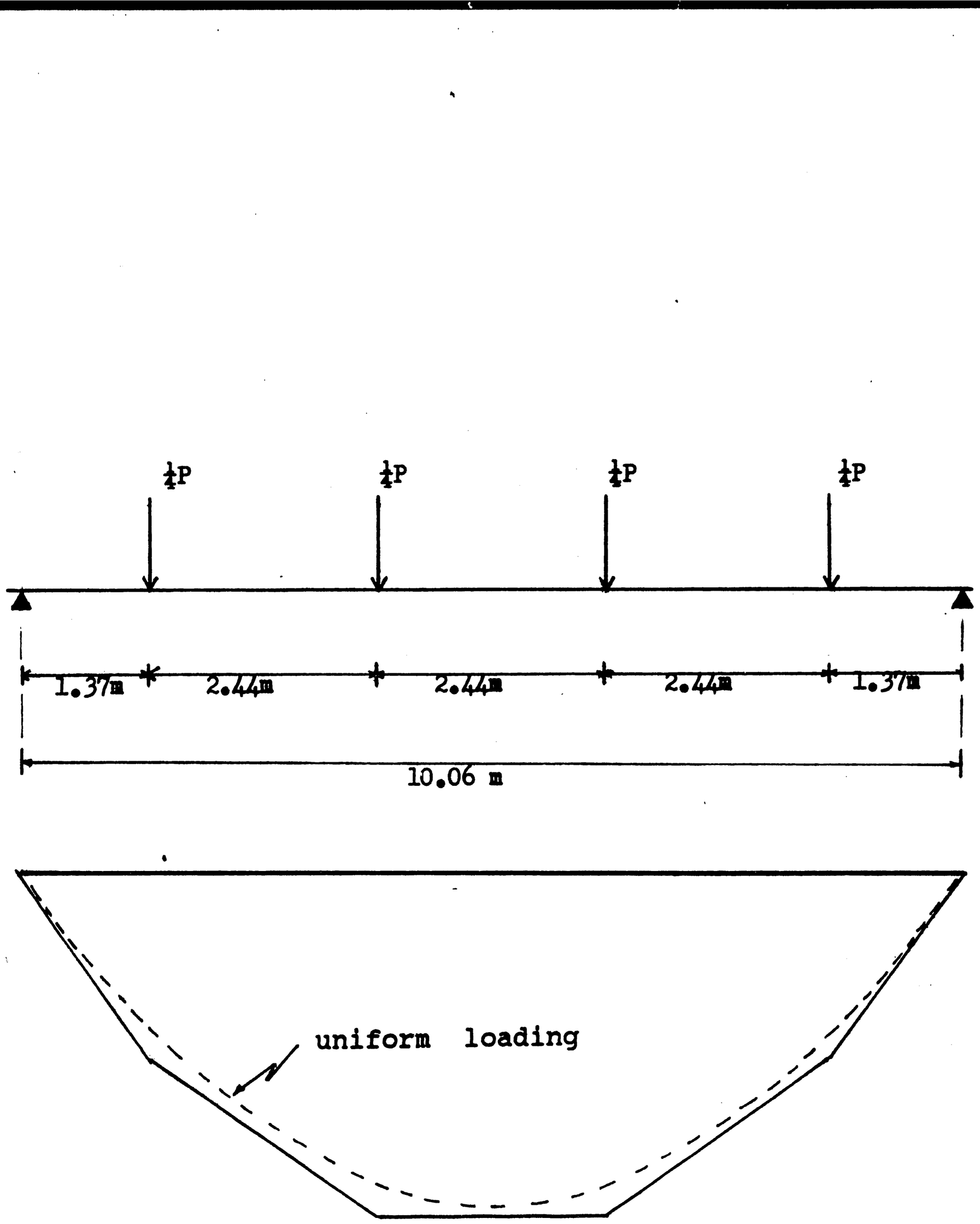

Figure 7: Moment Diagram Resulting From The Applied Loads

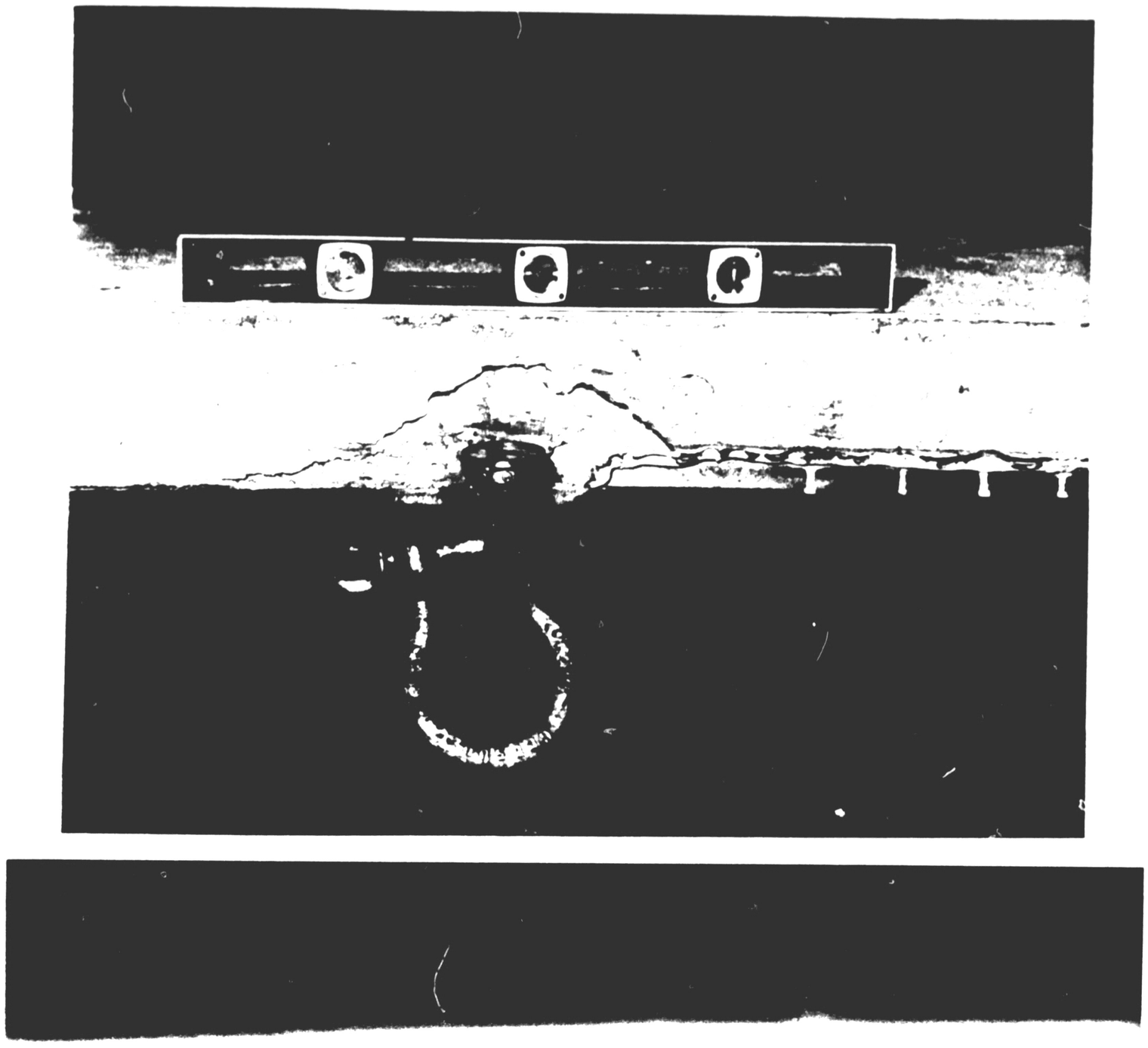

Figure 8: West End Crack At Conclusion of Test

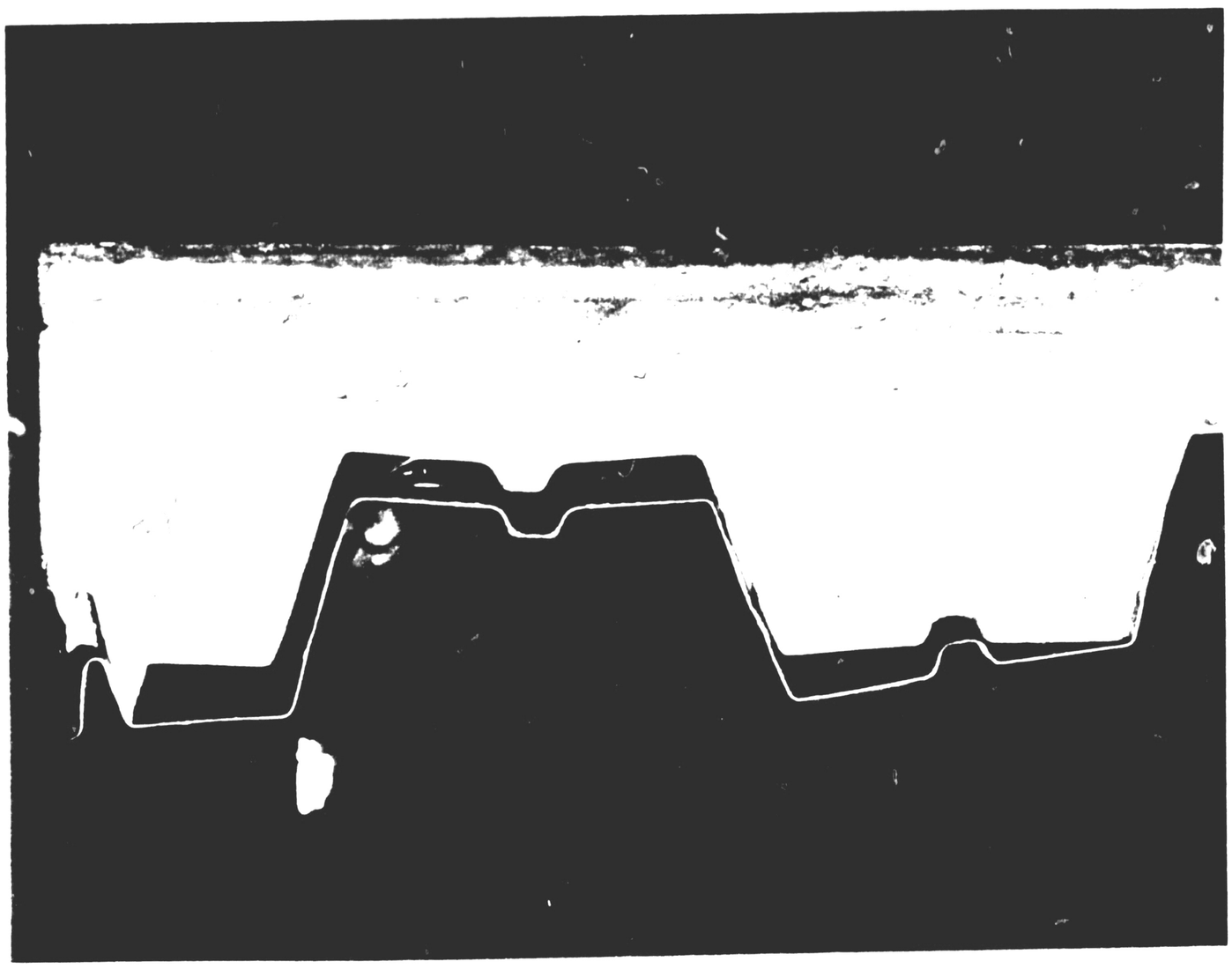

Figure 9: Separation of The Decking on The West End

Figure 10: Cellular Raceway Panel Before Test

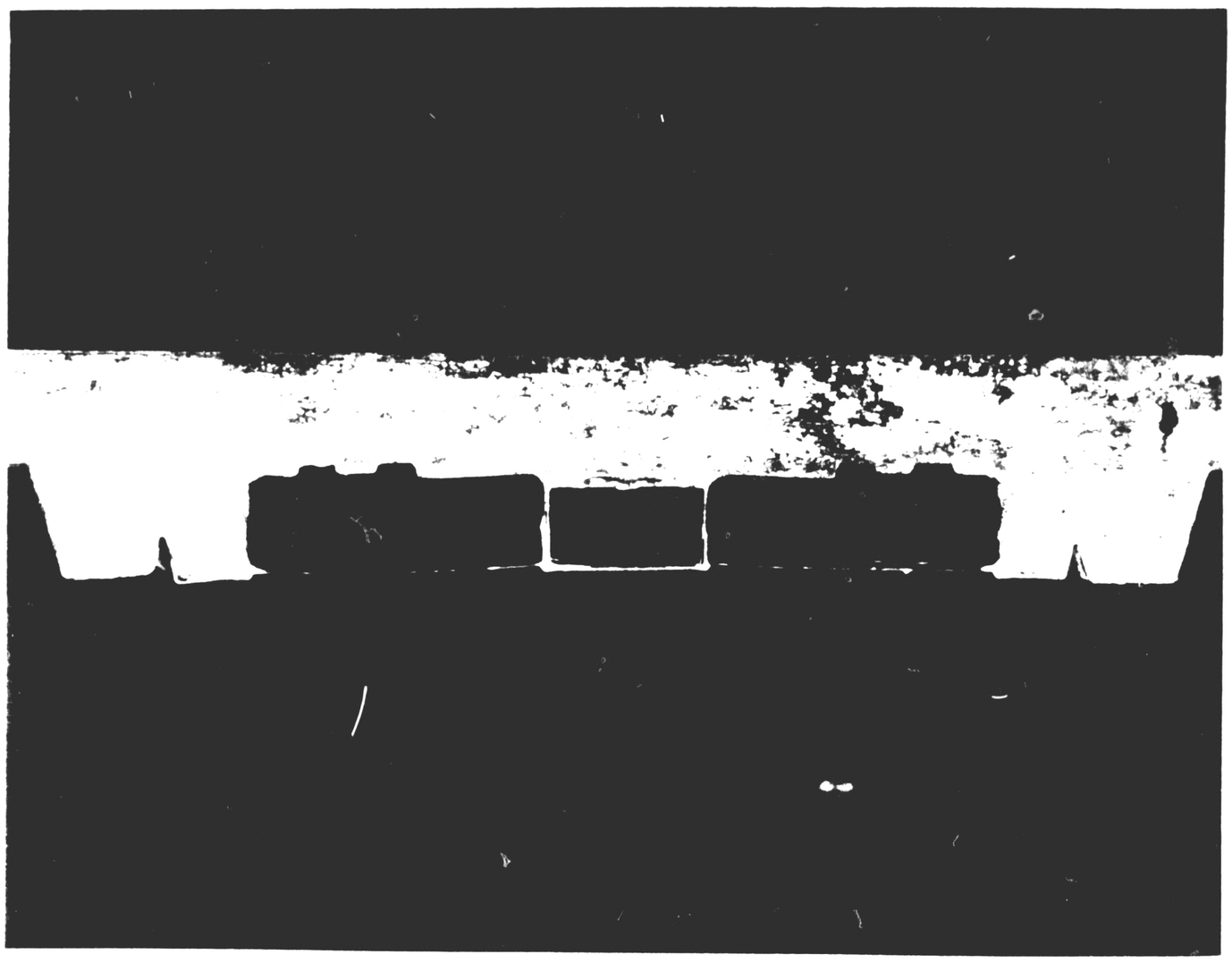

Figure 11: Cellular Raceway Panel After Test

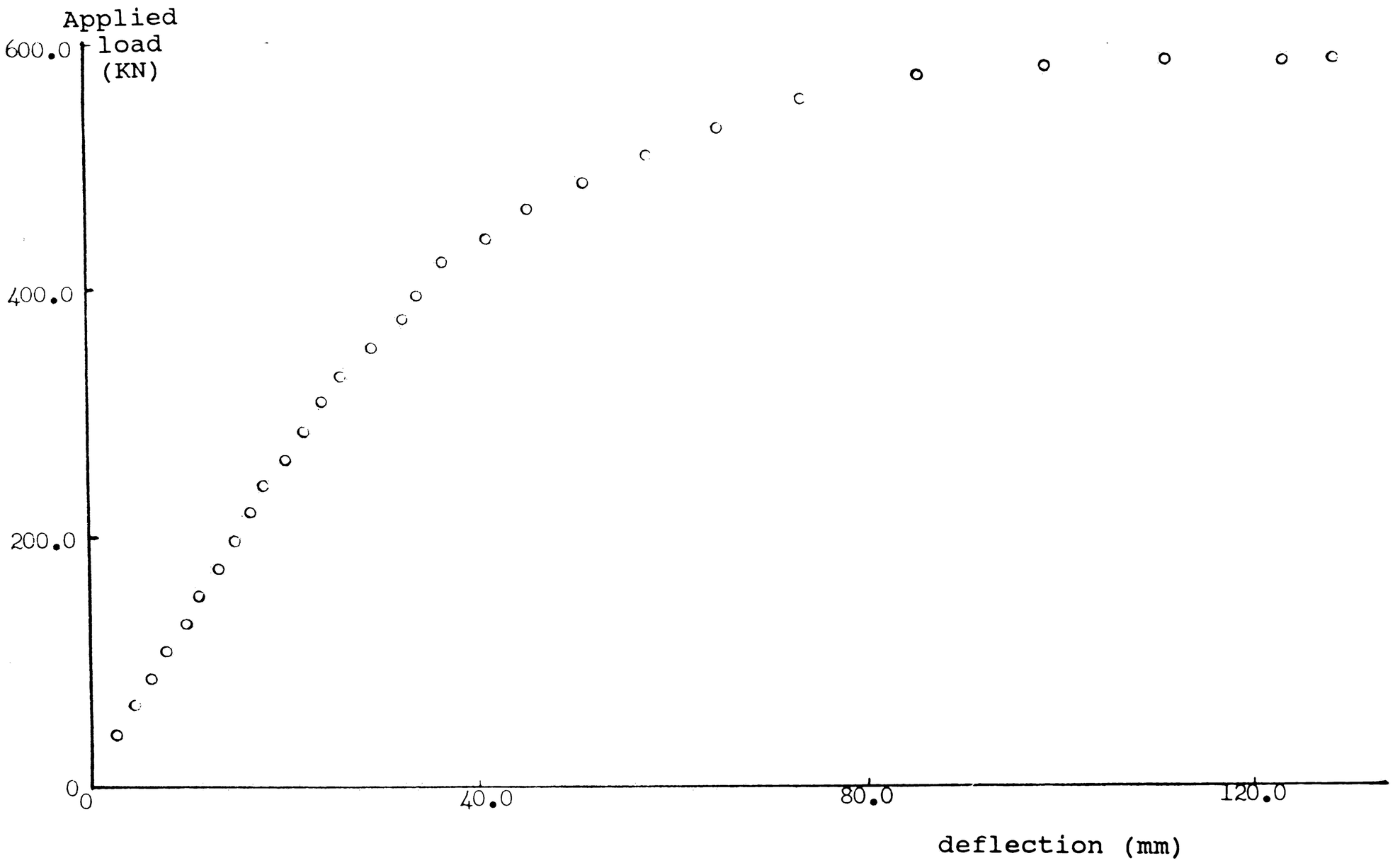

Figure 12: Applied Load vs. Mid-Span Deflection

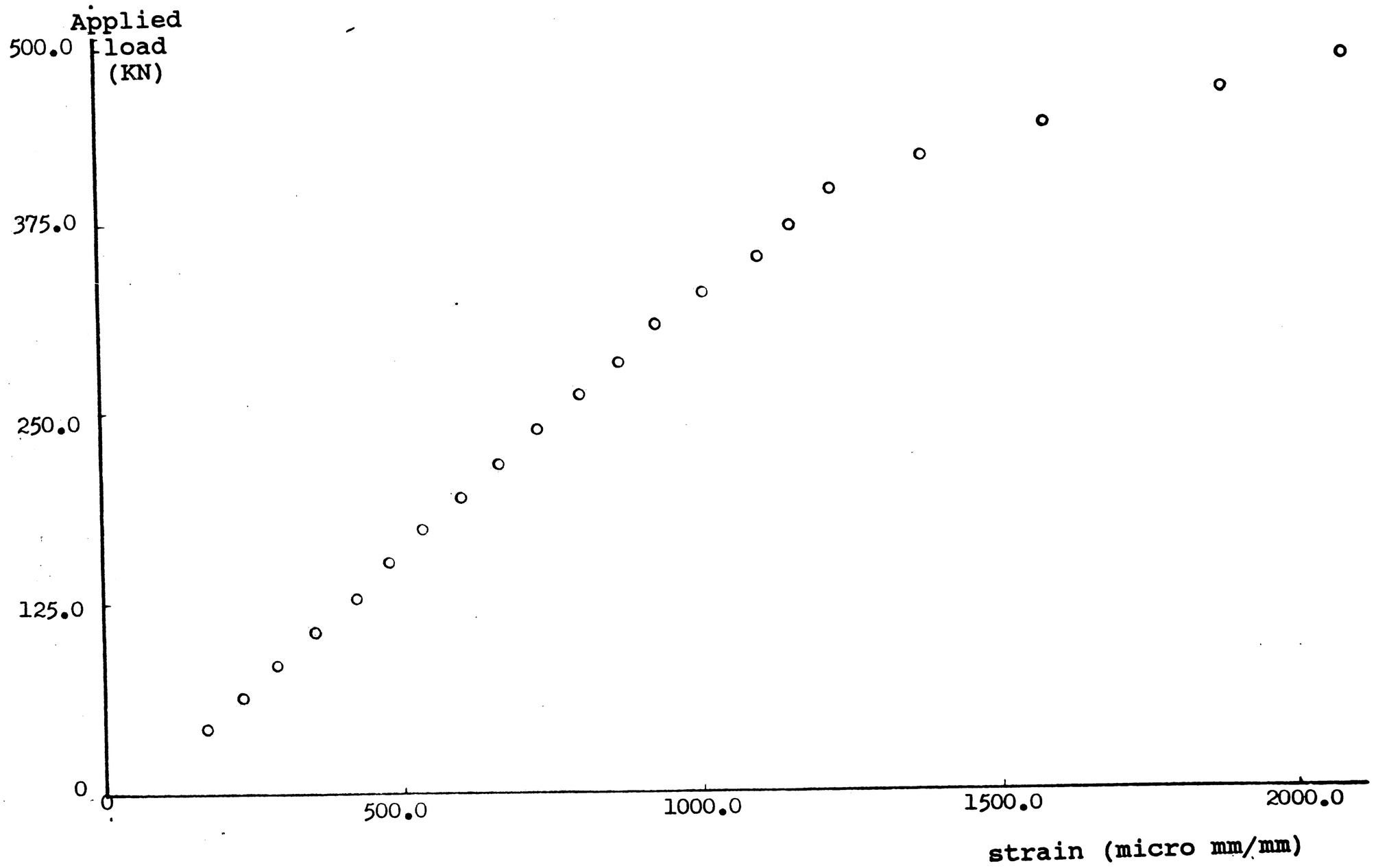

Figure 13: Applied Load vs. Bottom Flange Strain

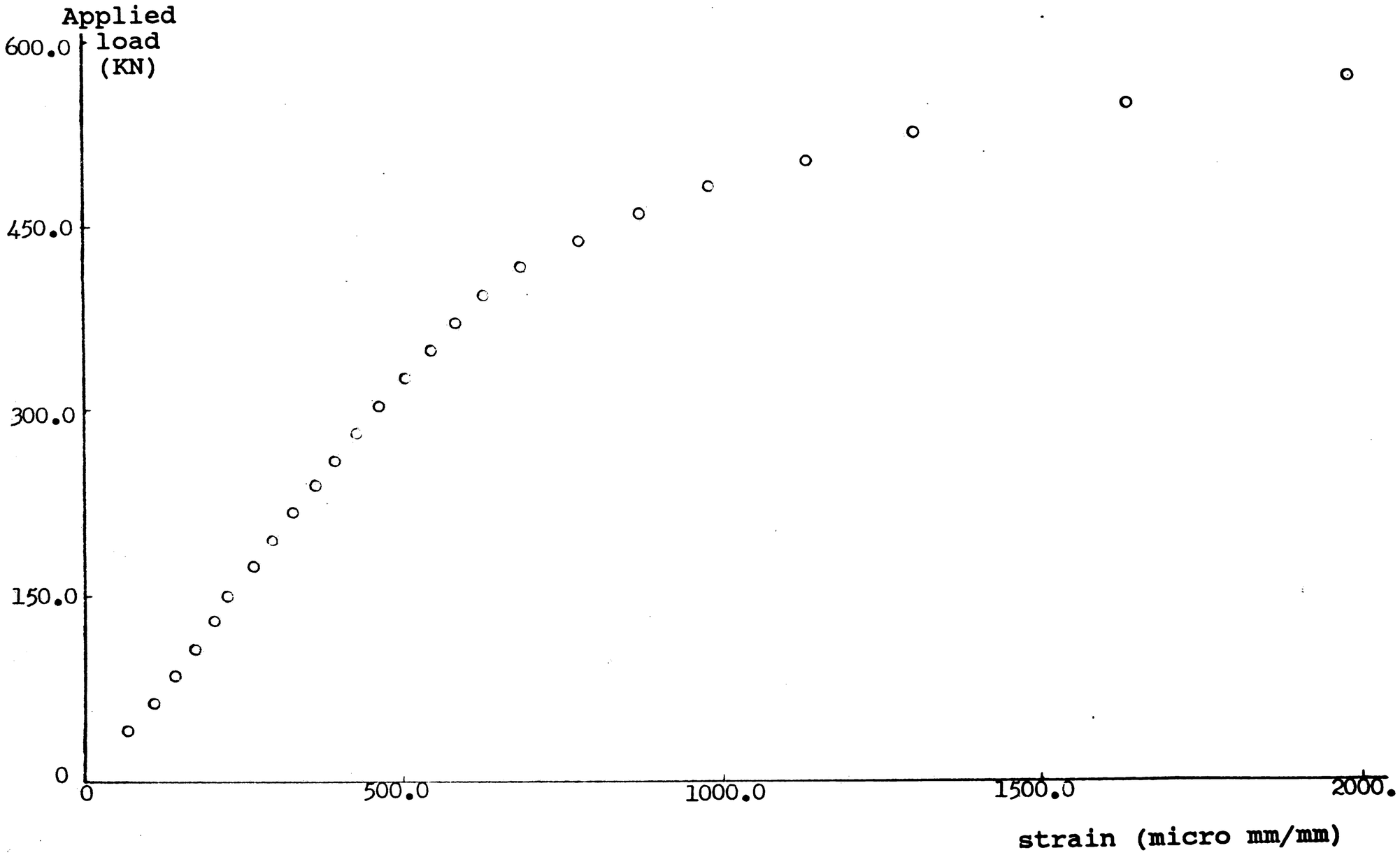

Figure 14: Applied Load vs. Mid-Height Web Strain

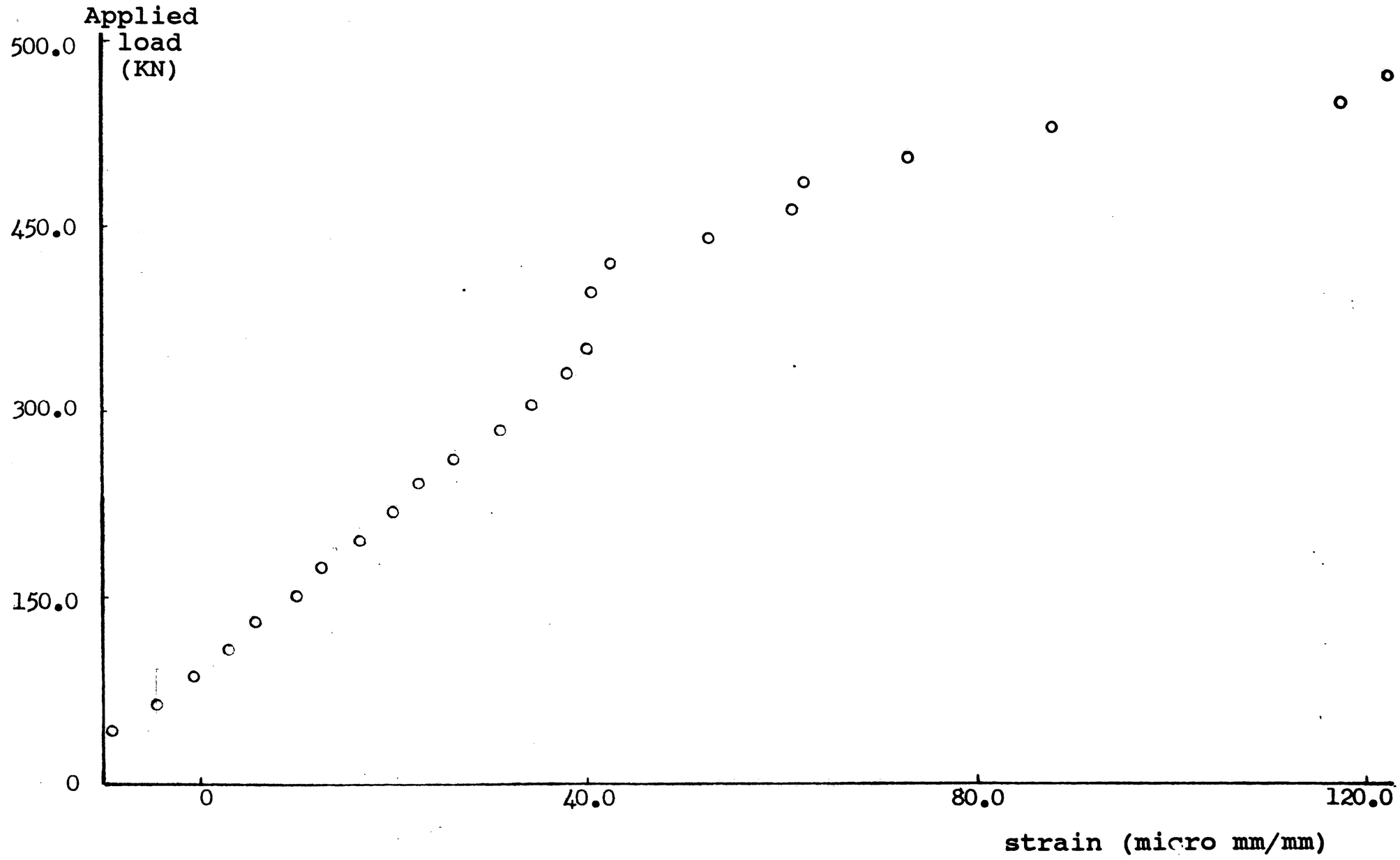

Figure 15: Applied Load vs. Top Flange Strain

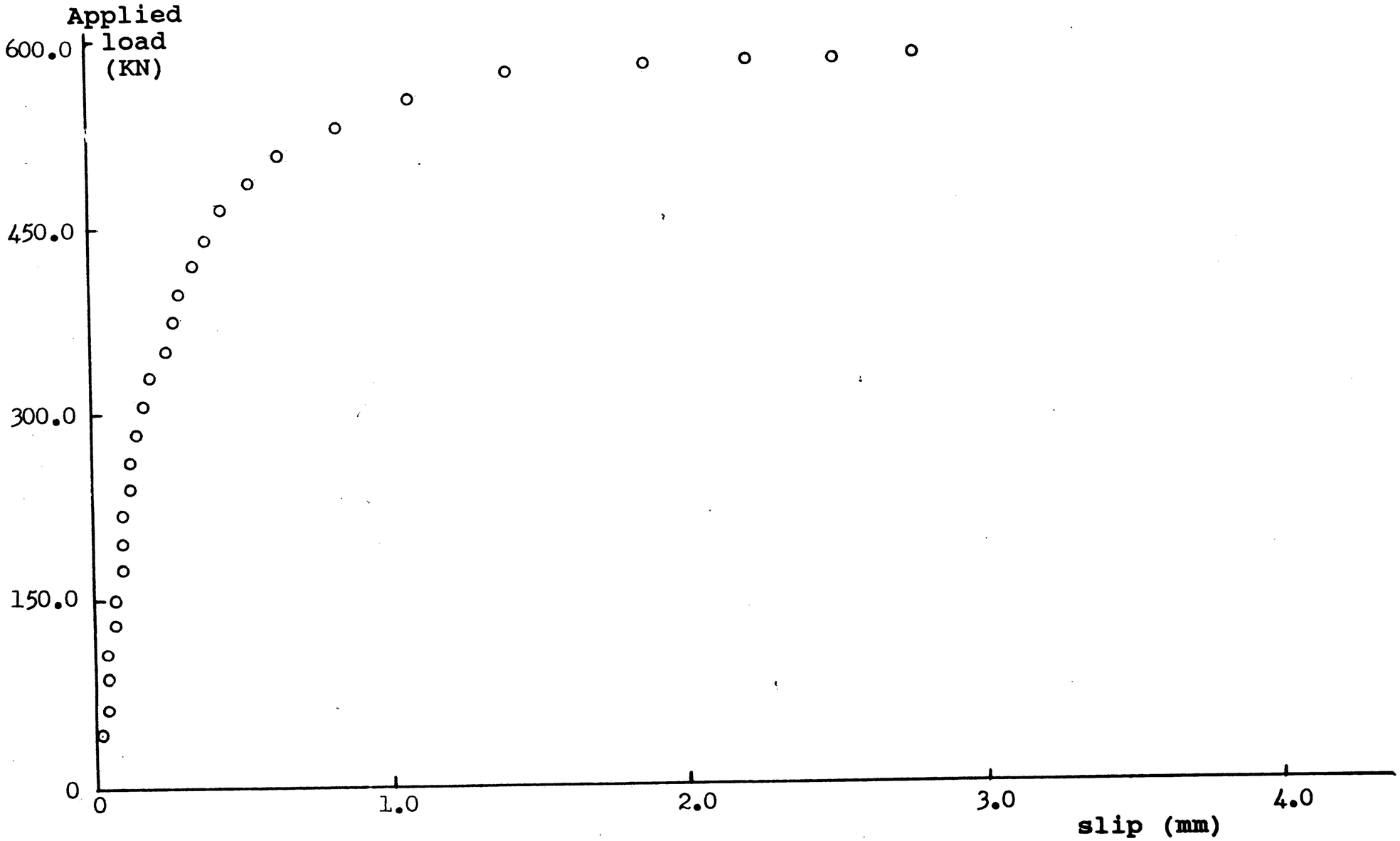

Figure 16: Applied Load vs. West End Slip

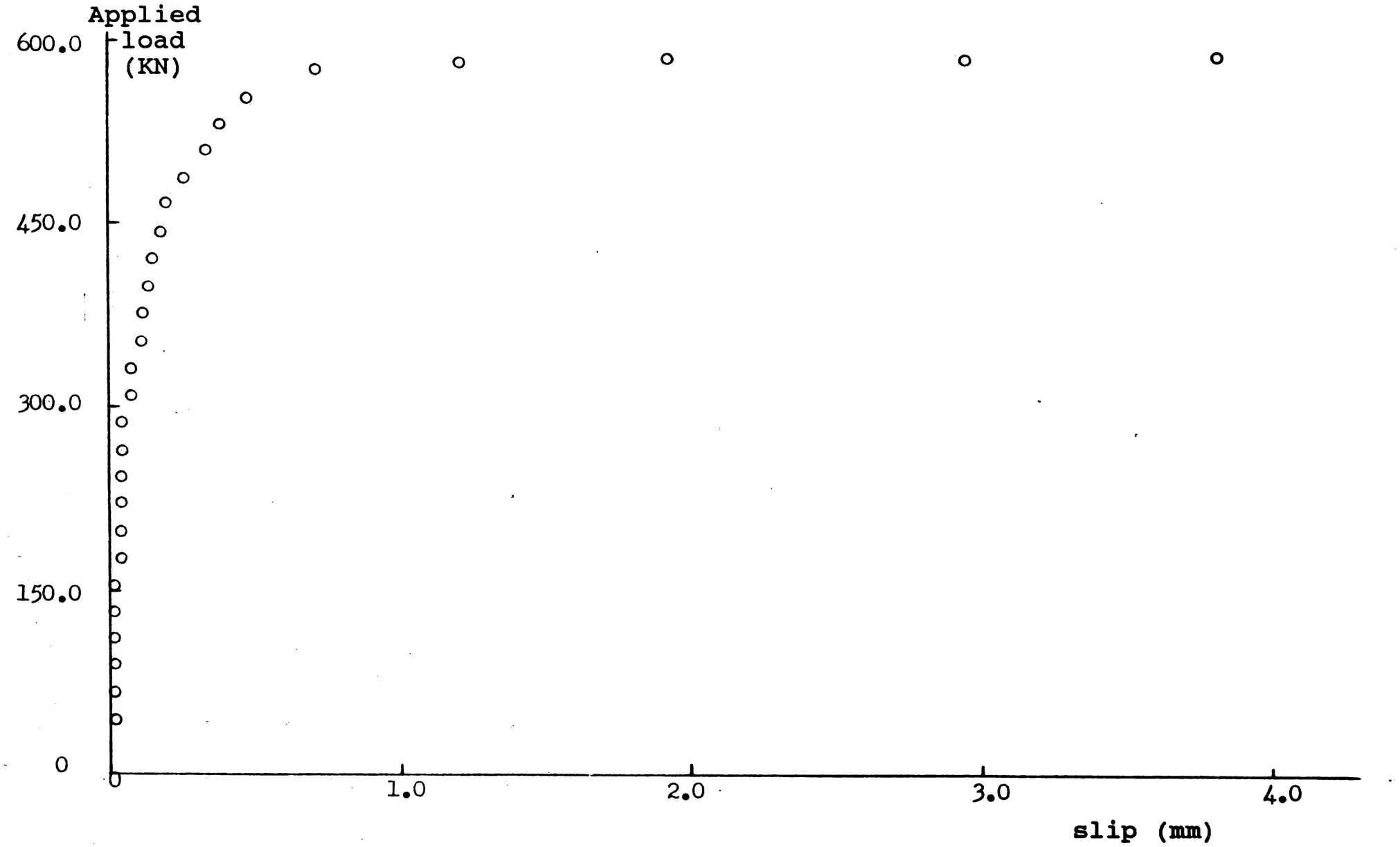

Figure 17: Applied Load vs. West Raceway Panel Slip

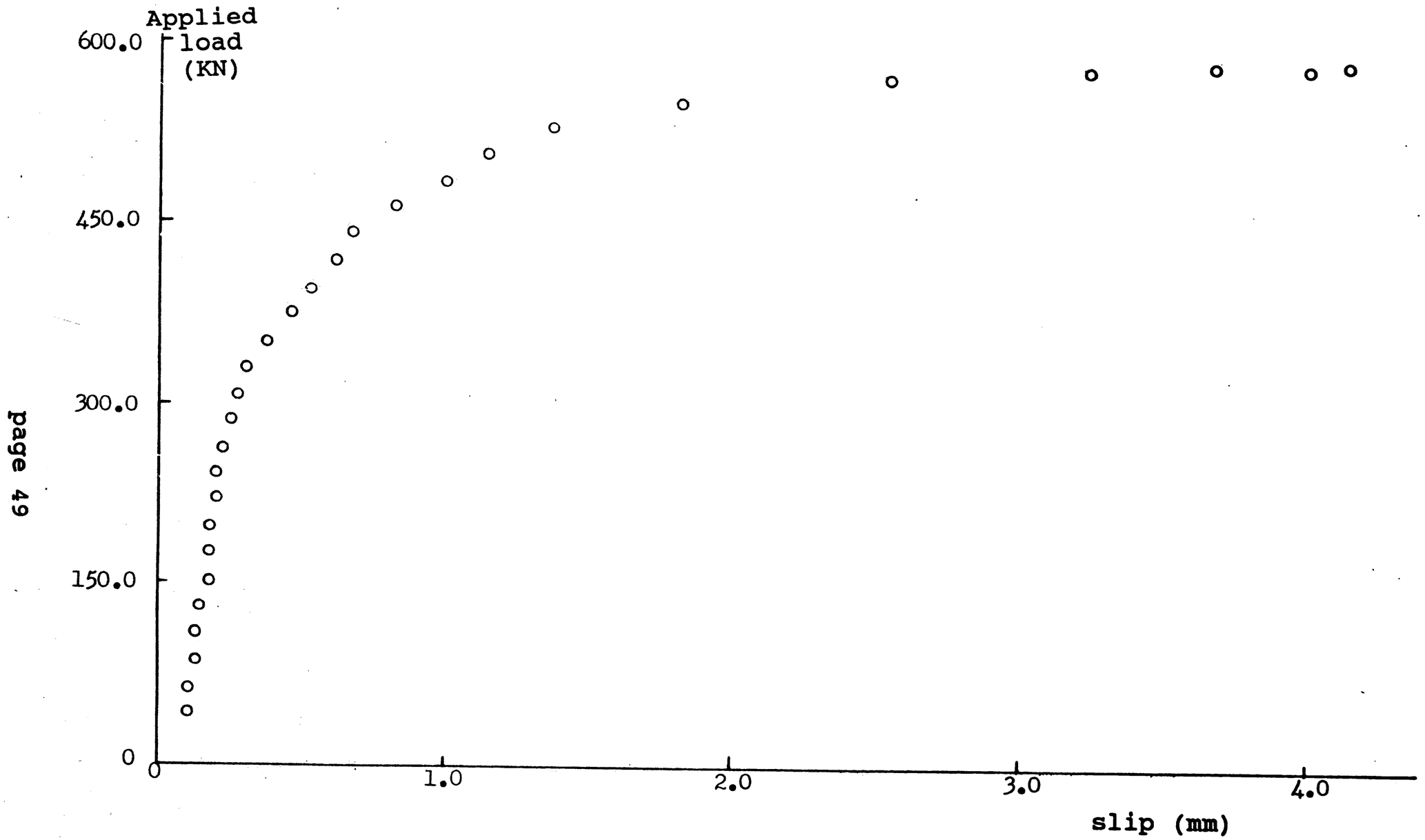

Figure 18: Applied Load vs. East End Slip

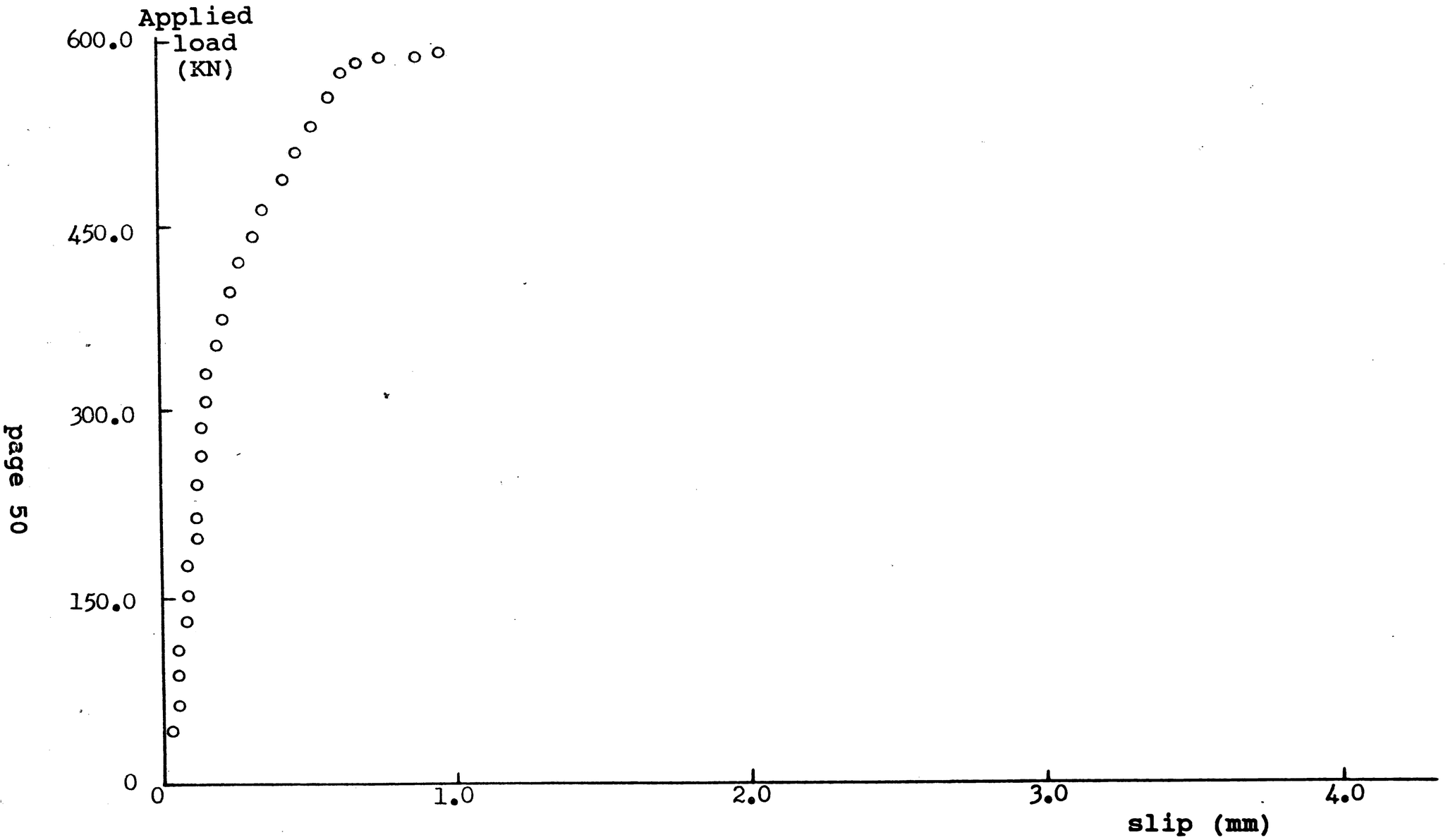

Figure 19: Applied Load vs. East Raceway Panel Slip

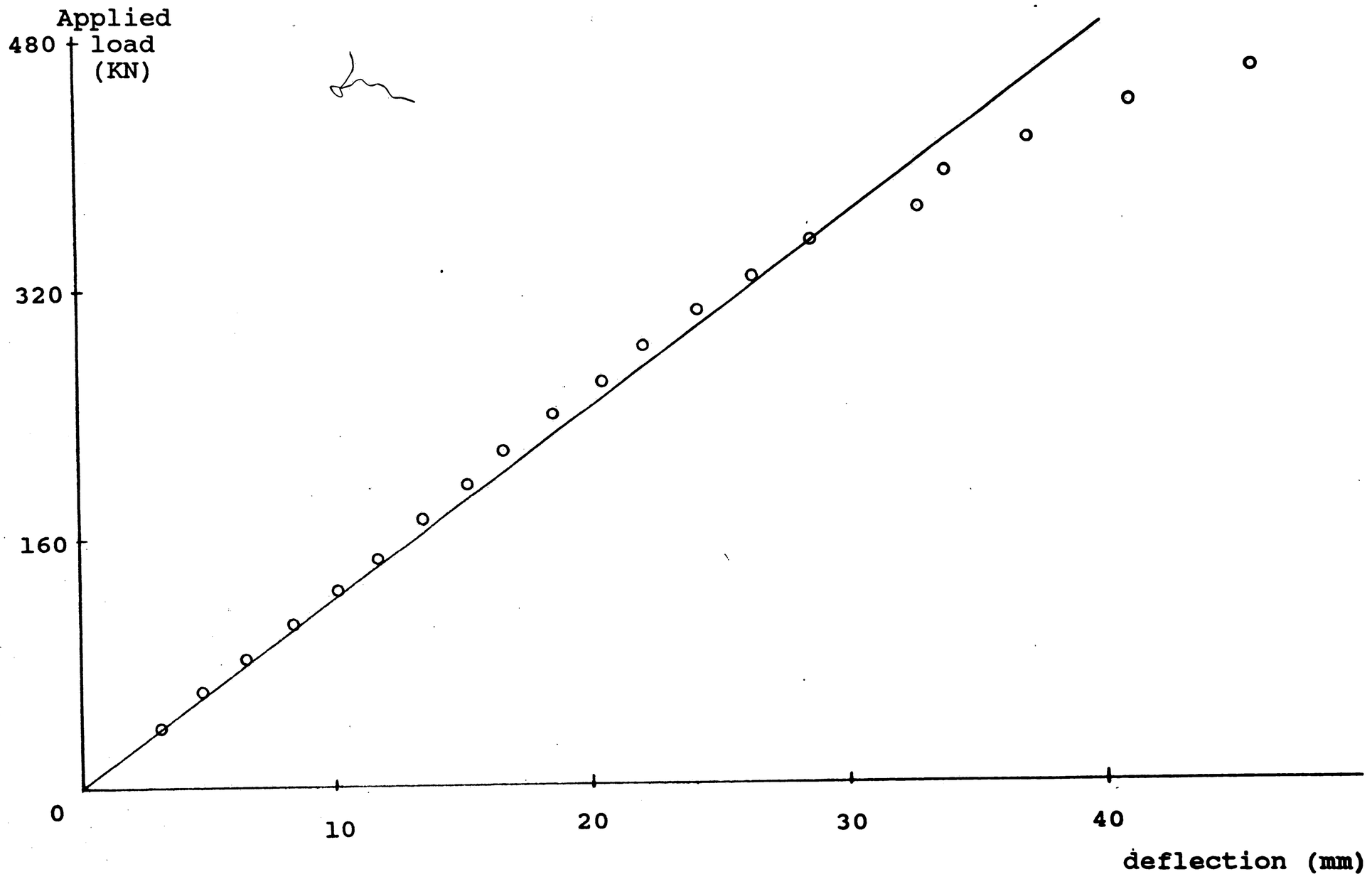

Figure 20: Theoretical Load Deflection Curve - Elastic Range

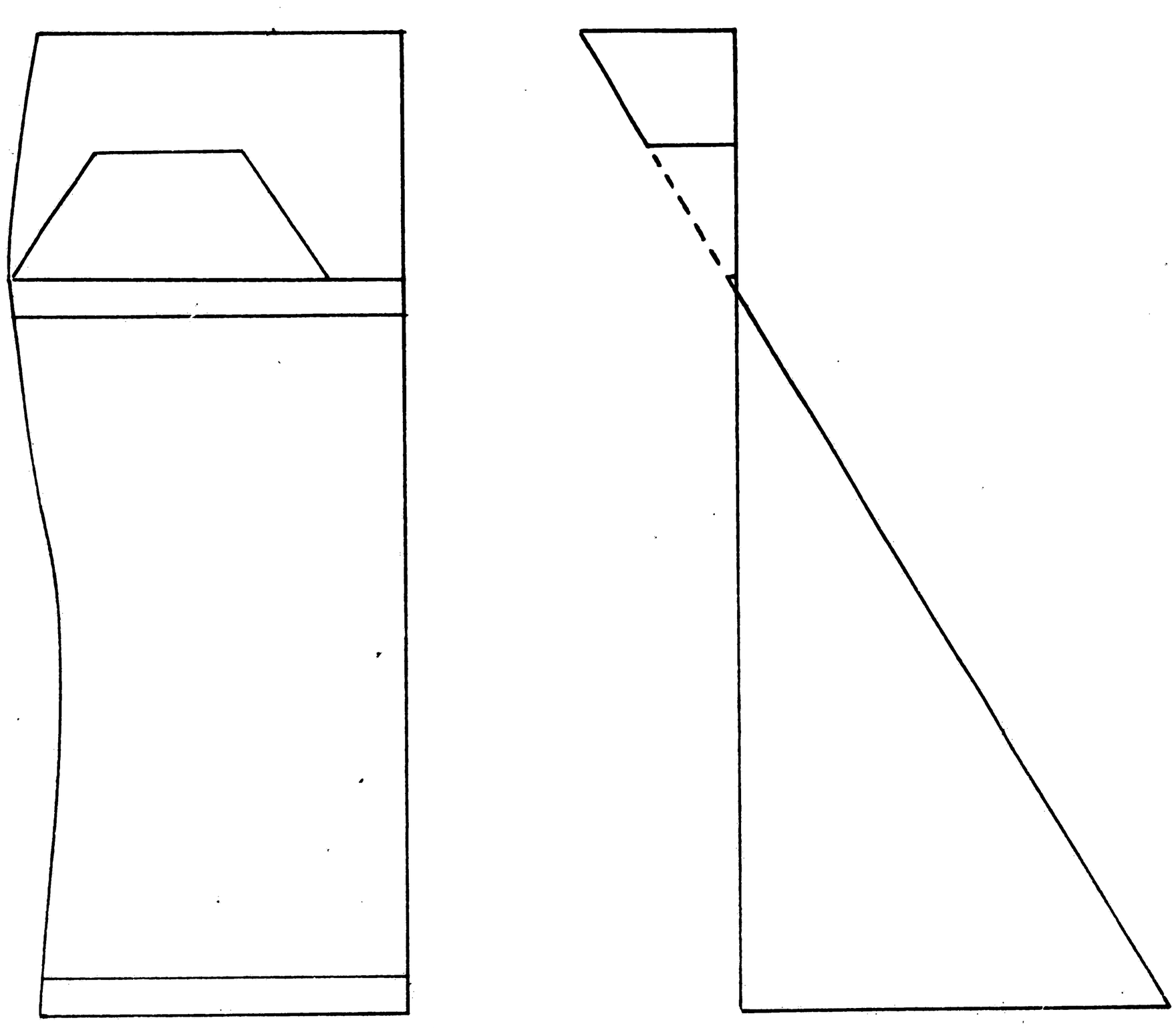

Figure 21: Typical Strain Profile

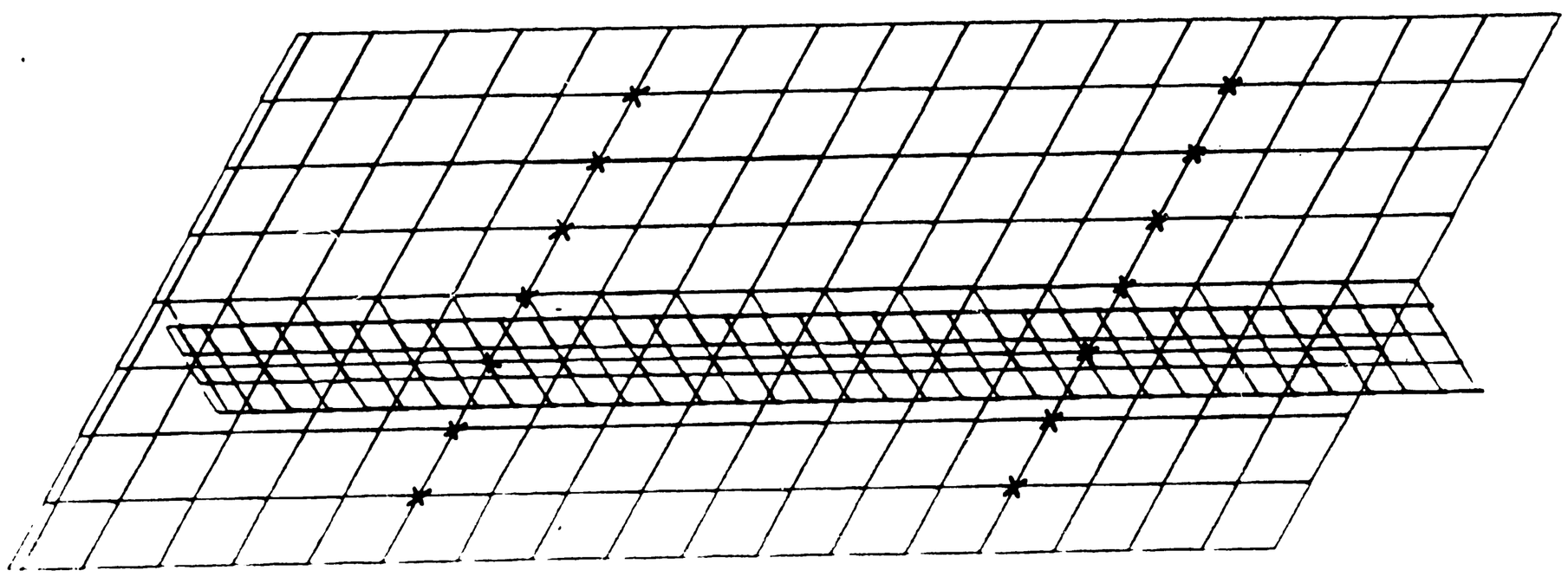

Figure 22: Finite Element Model

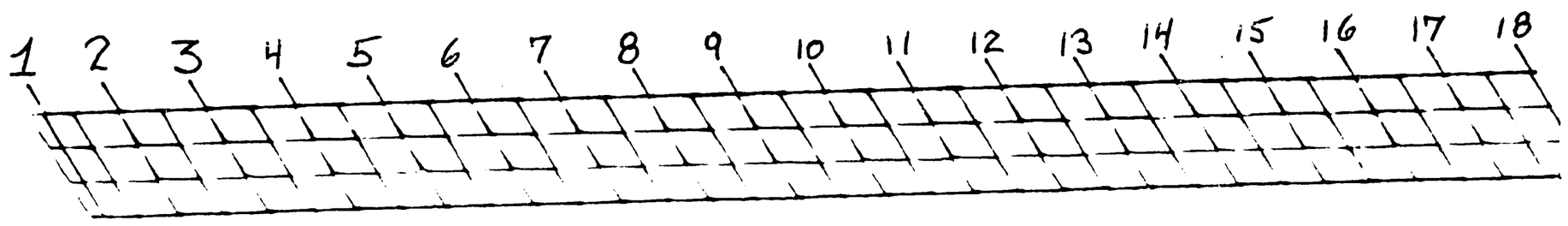

Figure 23: Finite Element Model With Slab Removed

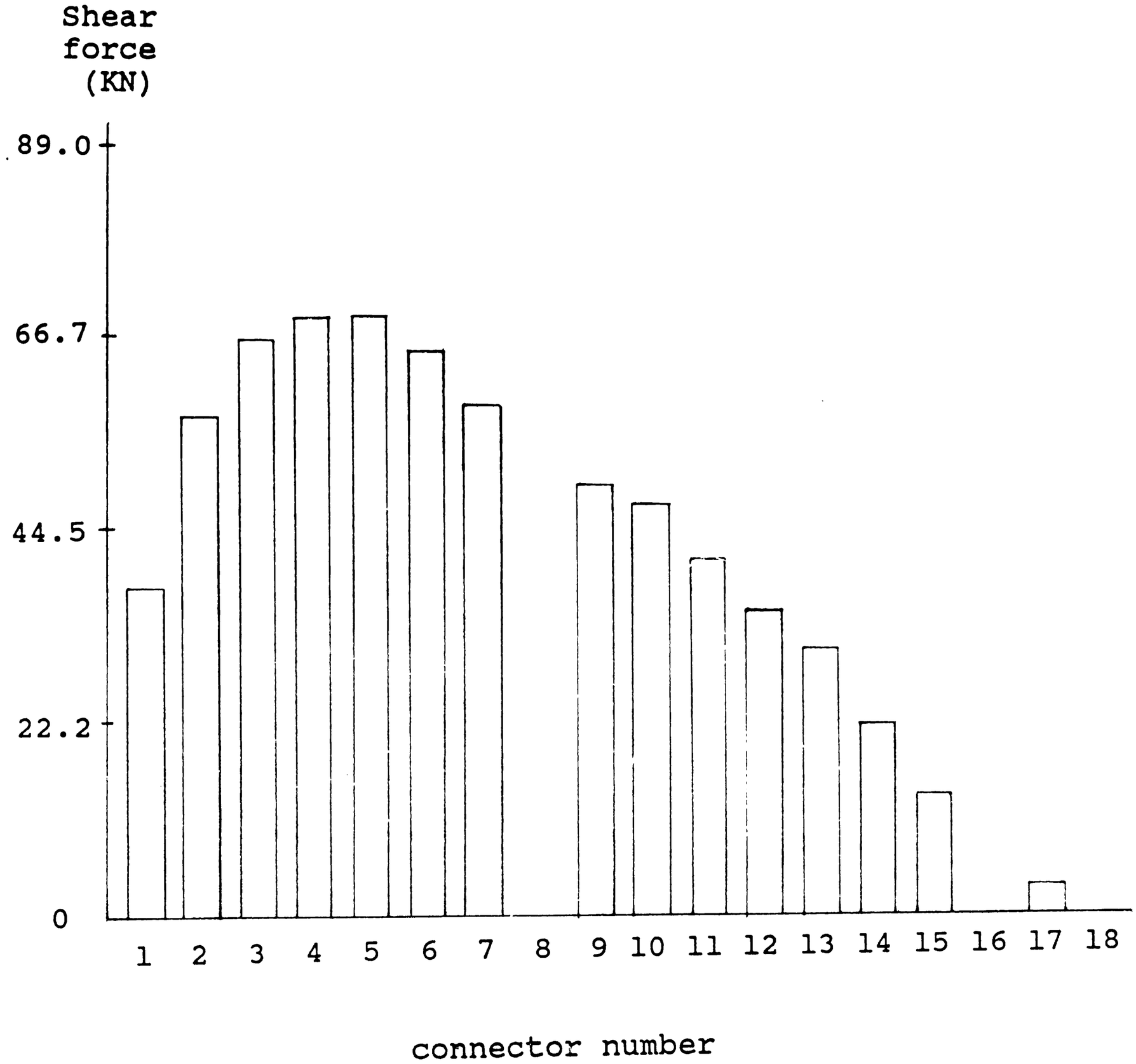

Figure 24:
Shear Force Distribution-Connectors 8 & 16 Removed

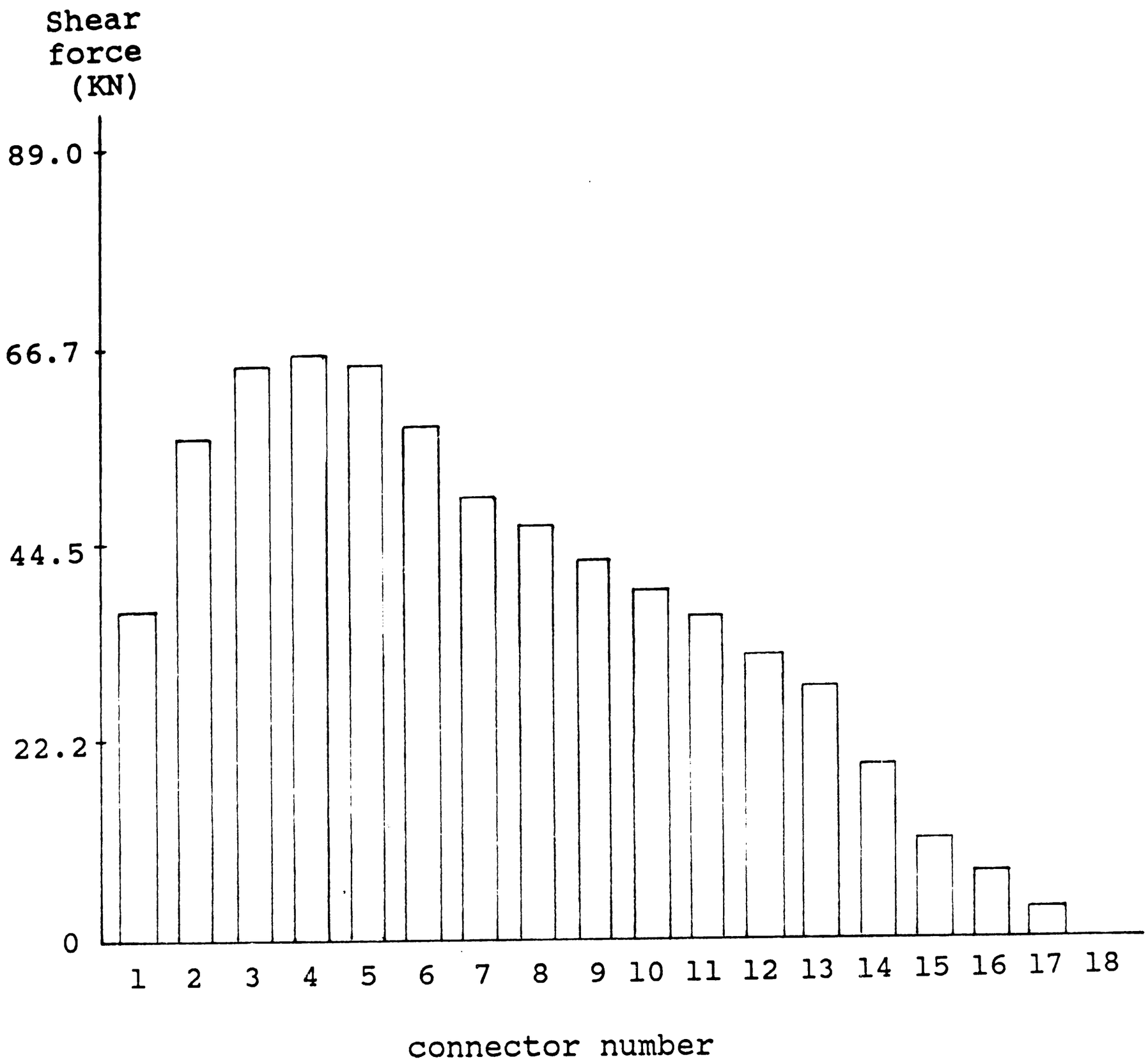

Figure 25: Shear Force distribution-No Missing Connectors

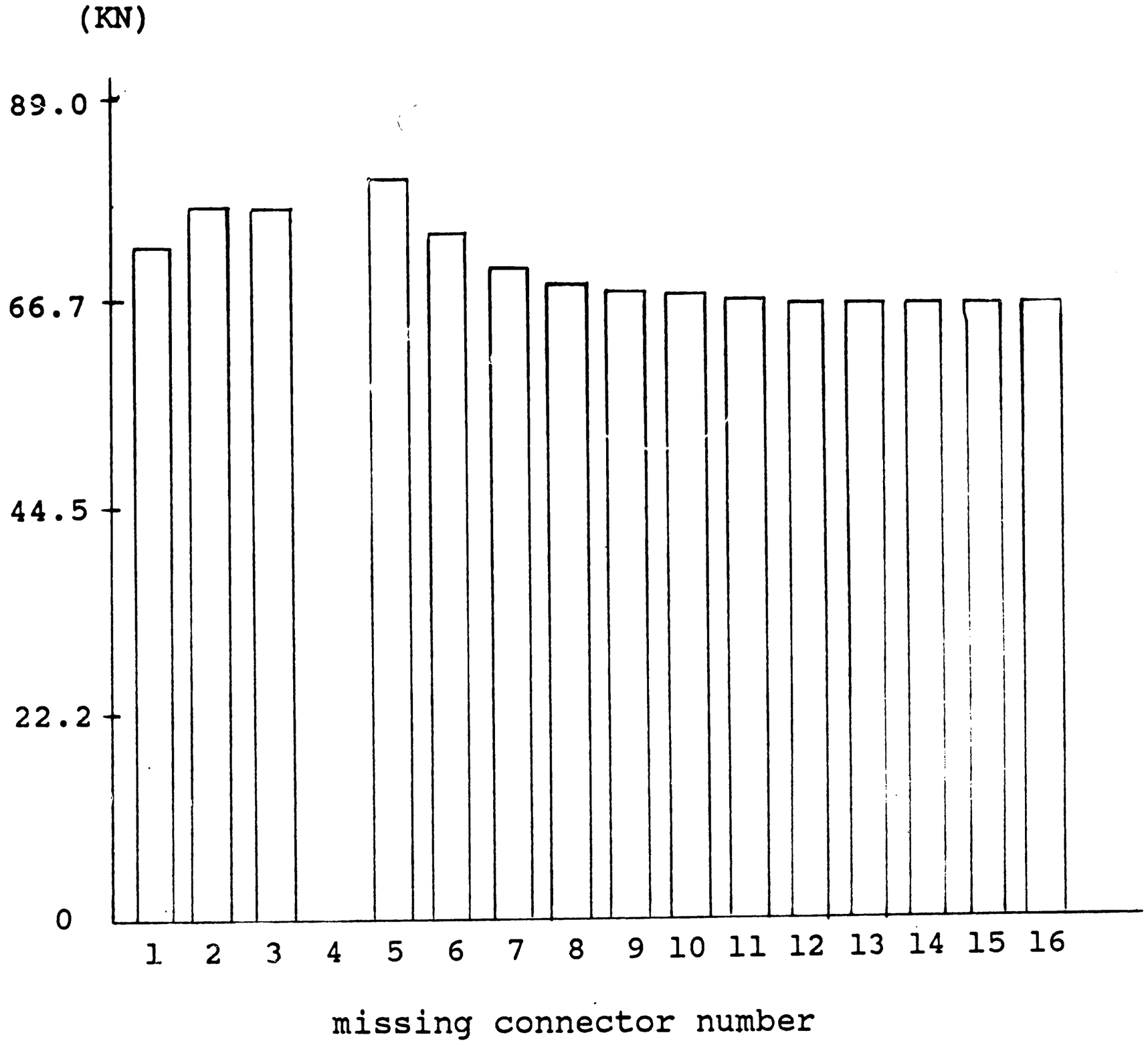

Figure 26: Shear Force on Connector 4 Resulting From The Removal of One Connector

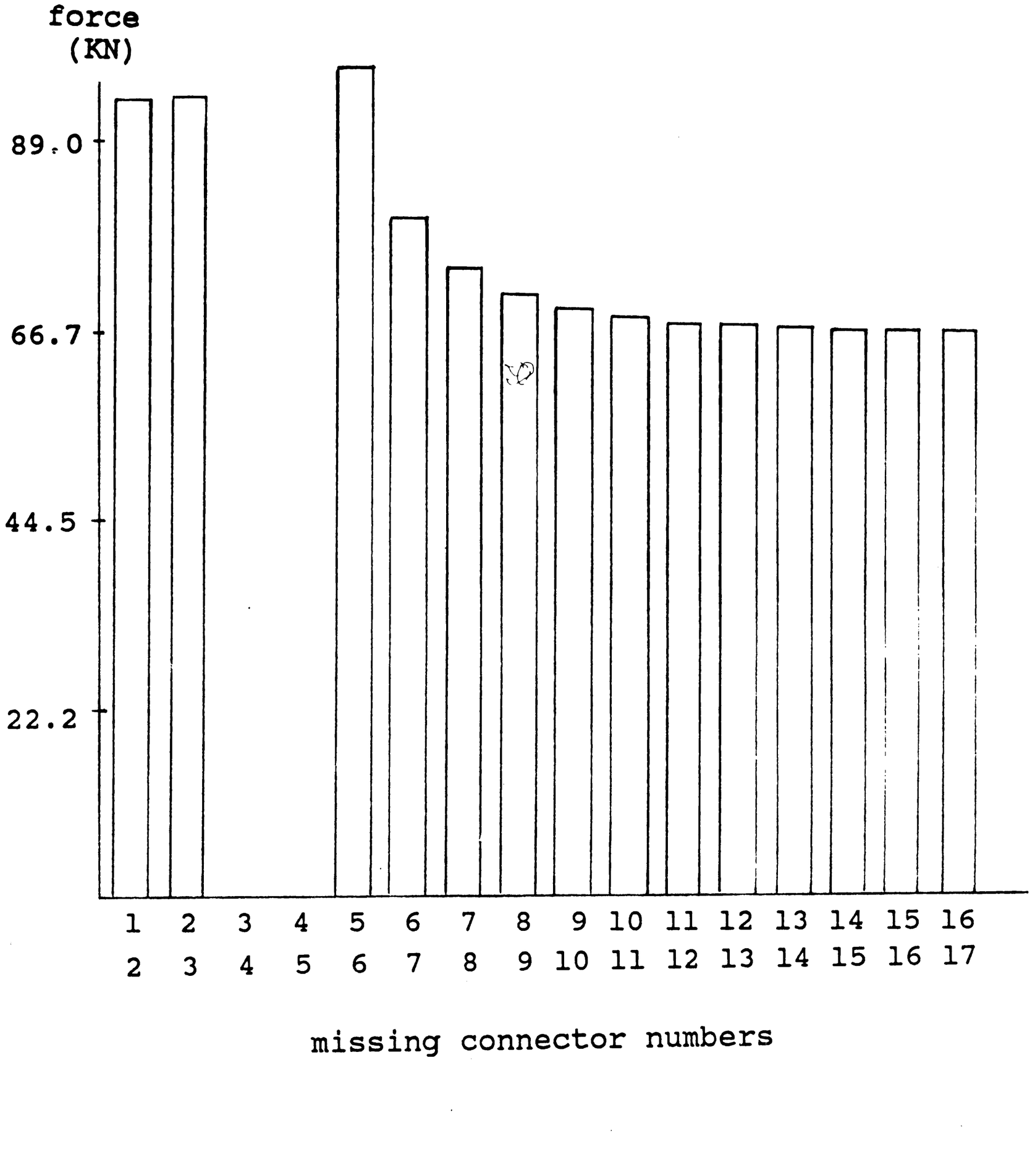

Figure 27: Shear Force on Connector 4 Resulting From The Removal of Two Connectors

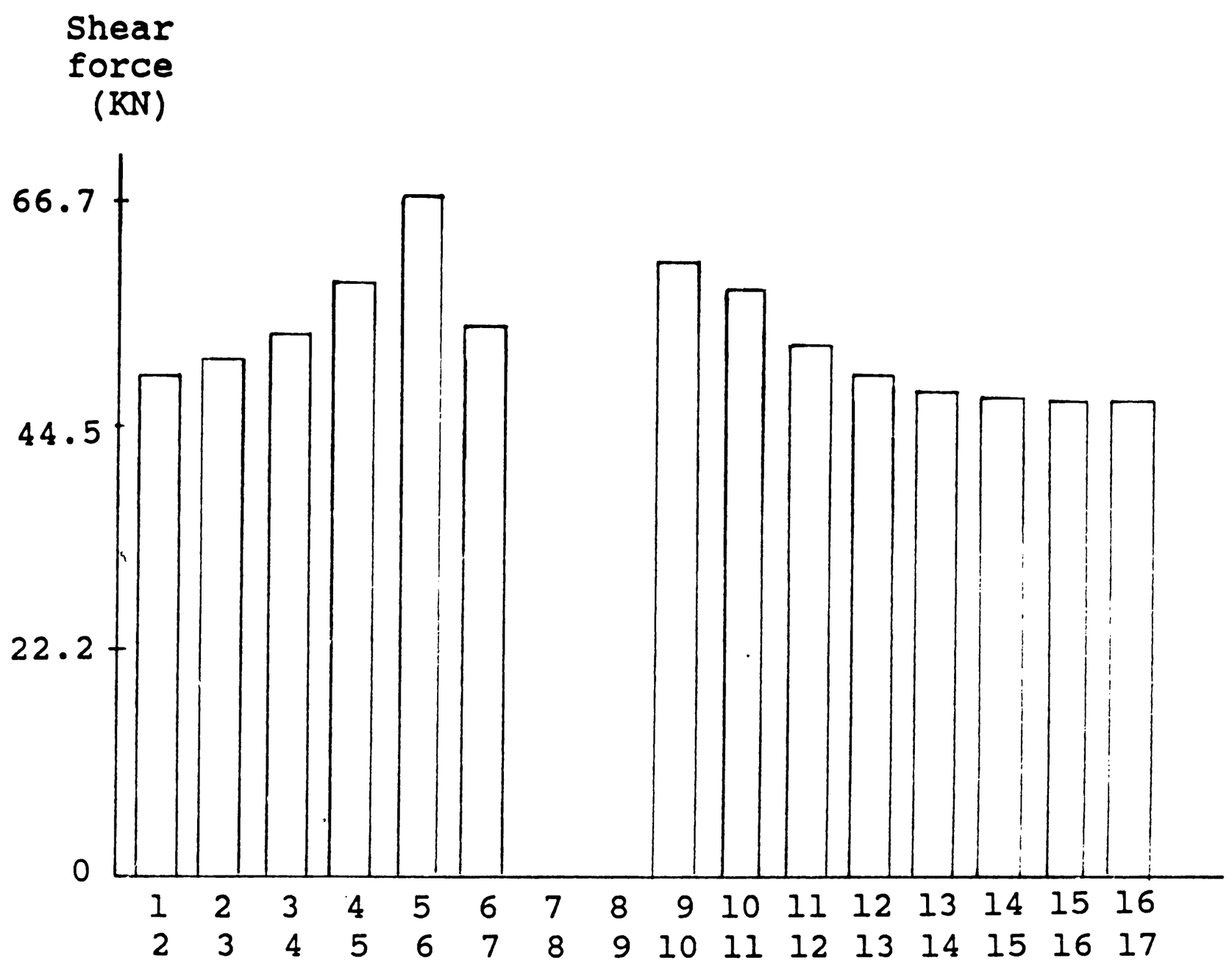

Figure 28: Shear Force on Connector 8 Resulting From The Removal of Two Connectors

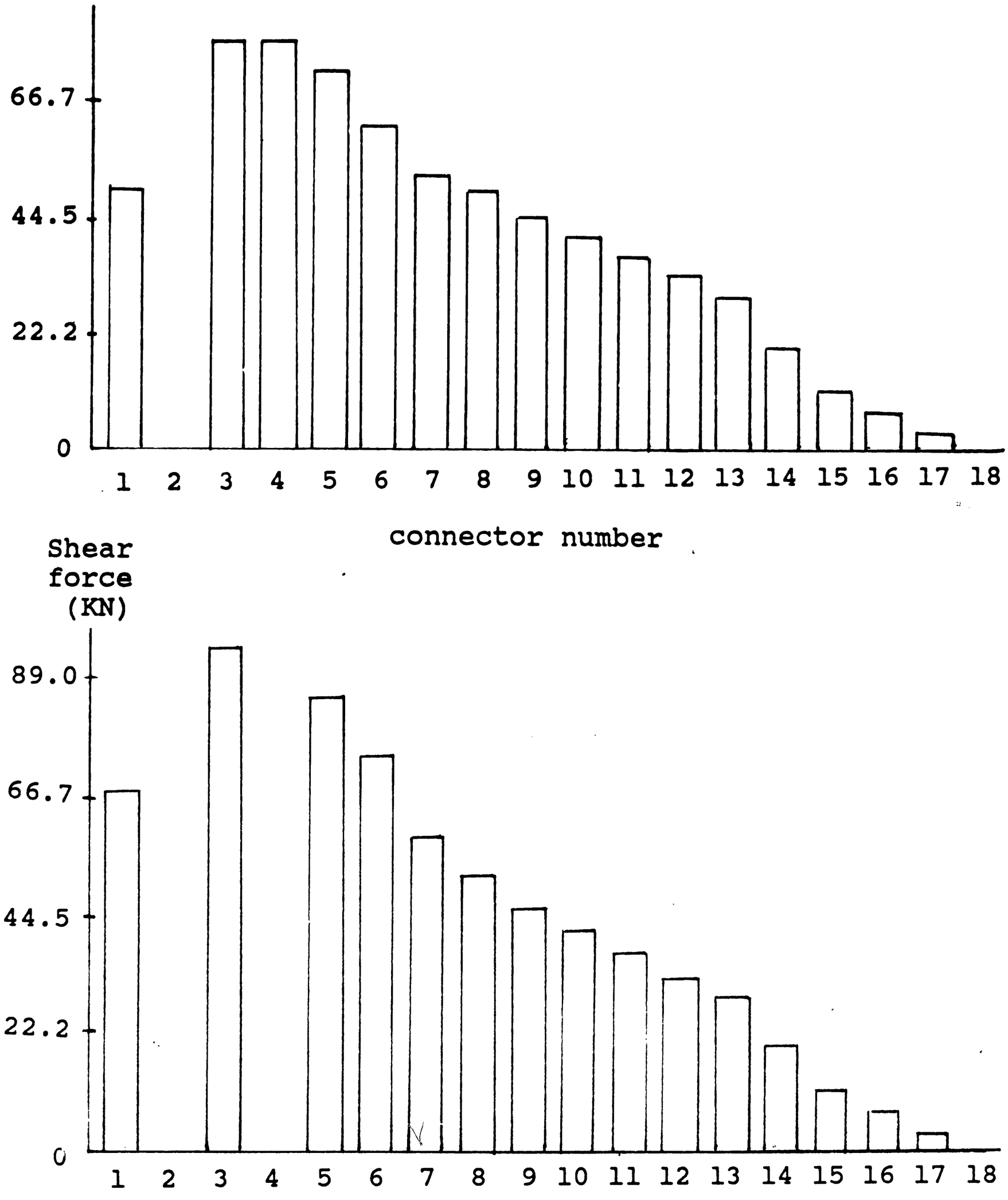

Figure 29: Shear Force distribution Resulting From The Removal of Connectors Near The Ends

8. REFERENCES

1. Robinson,Hugh,"Test of Composite Beams with Cellular Deck,"Journal of the Structural Division,ASCE,Vol.93 No.ST4,August 1967

2. Fisher,J.W.,"Design of Composite Beams with Formed Metal Deck,"Aisc Engineering Journal,AISC,Vol.7,No.3, July 1970

3. Grant,J.A.,Jr.,Fisher,J.W and Slutter,R.G.,"Composite Beams with Formed Steel Deck,"AISC Engineering Journal, AISC,Vol.14,No.1,January 1981

4. Grant,J.A.,Jr.,"Determination of Connector and Beam Behavior For Composite Beams With Deck Formed Slabs," Fritz Engineering Laboratory Report No.381.5,Lehigh University,Bethlehem,Pa.,January 1981

5. AISC,"Specification for the Design, Fabrication and Erection of Structural Steel for Buildings,"American Institute of Steel Construction Manual of Steel Construction,Eighth Edition,Chicago,1978

6. Slutter,R.G., and Driscoll,G.,"Flexural Strength of Steel Concrete Composite Beams,"Journal of the Structural division, ASCE,Vol.91,No.ST2,Proc.Paper 4294 April 1965

9. VITA

Joseph Marinaccio Jr. was born on July 2, 1962 in Mineola, New York. He is the son of Joseph Sr. and Joyce W Marinaccio.

He attended Old Dominion University in Norfolk, Virginia and graduated in May 1984 with a Bachelor of Science Degree in Civil Engineering. In September of the same year he enter the Graduate School of Lehigh University and was granted a Research Assistantship while working towards the degree of Master of Science in Civil Engineering.

He is a Student Member of the American Society of Civil Engineers and the American Concrete Institute.